

# [Ca<sup>2+</sup>]<sub>i</sub> oscillations in human sperm are triggered in the flagellum by membrane potential-sensitive activity of CatSper

Nitao, Elis; Brown, Sean; Mata-Martinez, Esperanza; Trevino, Claudia; Barratt, Christopher; Publicover, Steve

DOI:

[10.1093/humrep/deaa302](https://doi.org/10.1093/humrep/deaa302)

License:

None: All rights reserved

*Document Version*

Peer reviewed version

*Citation for published version (Harvard):*

Nitao, E, Brown, S, Mata-Martinez, E, Trevino, C, Barratt, C & Publicover, S 2020, '[Ca<sup>2+</sup>]<sub>i</sub> oscillations in human sperm are triggered in the flagellum by membrane potential-sensitive activity of CatSper', *Human Reproduction*. <https://doi.org/10.1093/humrep/deaa302>

[Link to publication on Research at Birmingham portal](#)

## **Publisher Rights Statement:**

This is a pre-copyedited, author-produced version of an article accepted for publication in *Human Reproduction* following peer review. The version of record, Elis Torrezan-Nitao, Sean G Brown, Esperanza Mata-Martínez, Claudia L Treviño, Christopher Barratt, Stephen Publicover, [Ca<sup>2+</sup>]<sub>i</sub> oscillations in human sperm are triggered in the flagellum by membrane potential-sensitive activity of CatSper, *Human Reproduction*, , deaa302, is available online at: <https://doi.org/10.1093/humrep/deaa302>

## **General rights**

Unless a licence is specified above, all rights (including copyright and moral rights) in this document are retained by the authors and/or the copyright holders. The express permission of the copyright holder must be obtained for any use of this material other than for purposes permitted by law.

- Users may freely distribute the URL that is used to identify this publication.
- Users may download and/or print one copy of the publication from the University of Birmingham research portal for the purpose of private study or non-commercial research.
- User may use extracts from the document in line with the concept of 'fair dealing' under the Copyright, Designs and Patents Act 1988 (?)
- Users may not further distribute the material nor use it for the purposes of commercial gain.

Where a licence is displayed above, please note the terms and conditions of the licence govern your use of this document.

When citing, please reference the published version.

## **Take down policy**

While the University of Birmingham exercises care and attention in making items available there are rare occasions when an item has been uploaded in error or has been deemed to be commercially or otherwise sensitive.

If you believe that this is the case for this document, please contact [UBIRA@lists.bham.ac.uk](mailto:UBIRA@lists.bham.ac.uk) providing details and we will remove access to the work immediately and investigate.



Draft Manuscript For Review. Reviewers should submit their review at <http://mc.manuscriptcentral.com/humrep>

## **[Ca<sup>2+</sup>]<sub>i</sub> oscillations in human sperm are triggered in the flagellum by membrane potential-sensitive activity of CatSper**

Journal:	<i>Human Reproduction</i>
Manuscript ID	HUMREP-20-1008.R1
Manuscript Type:	Original Article
Date Submitted by the Author:	n/a
Complete List of Authors:	Torrezan-Nitao, Elis; School of Biological Science, University of Birmingham Brown, Sean; University of Abertay, Mata-Martinez, Esperanza; Universidad Nacional Autónoma de México Campus Morelos, Departamento de Genética del Desarrollo y Fisiología Molecular Trevino, Claudia; Instituto de Biotecnología, Genética del Desarrollo y Fisiología Molecular Barratt, C; University of Dundee, Maternal & Child Health Sciences; Publicover, Stephen; School of Biological Science, University of Birmingham
Keywords:	sperm, Ca <sup>2+</sup> oscillation, CatSper, membrane potential, RU1968
Subject Section:	Andrology
Note: The following files were submitted by the author for peer review, but cannot be converted to PDF. You must view these files (e.g. movies) online.	
video 1.avi video 2.avi video 3.avi video 4.avi video 5.avi video 6.avi video 7.avi	

SCHOLARONE™  
Manuscripts

1  
2  
3  
4  
5  
6  
7  
8  
9  
10  
11  
12  
13  
14  
15  
16  
17  
18  
19  
20  
21

[Ca<sup>2+</sup>]<sub>i</sub> oscillations in human sperm are triggered in the flagellum by membrane potential-sensitive activity of CatSper

<sup>1</sup>Elis Torrezan-Nitao, <sup>2</sup>Sean G. Brown, <sup>3</sup>Esperanza Mata-Martínez, <sup>3</sup>Claudia L. Treviño, <sup>4</sup>Christopher Barratt, and <sup>1</sup>Stephen Publicover

<sup>1</sup>School of Biosciences, University of Birmingham, Birmingham

<sup>2</sup>School of Applied Sciences, Abertay University, Dundee DD11HG, UK

<sup>3</sup>Departamento de Genética del Desarrollo y Fisiología Molecular, Instituto de Biotecnología, Universidad Nacional Autónoma de México, Cuernavaca, Morelos 62210, México

<sup>4</sup>Systems Medicine, Ninewells Hospital and Medical School, University of Dundee, Dundee, DD19SY, UK

Running title: Vm and CatSper trigger sperm Ca<sup>2+</sup> oscillations

Key words: sperm, Ca<sup>2+</sup> oscillation, CatSper, membrane potential, RU1968

## 22 Abstract

23 **Study question:** How are progesterone (P4)-induced repetitive intracellular  $\text{Ca}^{2+}$  concentration  
24 ( $[\text{Ca}^{2+}]_i$ ) signals (oscillations) in human sperm generated?

25 **Summary answer:** P4-induced  $[\text{Ca}^{2+}]_i$  oscillations are generated in the flagellum by membrane-  
26 potential ( $V_m$ )-dependent  $\text{Ca}^{2+}$ -influx through CatSper channels, which then induce secondary  $\text{Ca}^{2+}$   
27 mobilisation at the sperm head/neck region.

28 **What is known already:** A subset of human sperm display  $[\text{Ca}^{2+}]_i$  oscillations that regulate flagellar  
29 beating and acrosome reaction. Though pharmacological manipulations indicate involvement of  
30 stored  $\text{Ca}^{2+}$  in these oscillations, influx of extracellular  $\text{Ca}^{2+}$  is also required.

31 **Study design, size, duration:** This was a laboratory study, that used >20 sperm donors and involved  
32 more than 100 separate experiments and analysis of more than 1,000 individual cells over a period of  
33 2 years.

34 **Participants/materials, setting, methods:** Semen donors and patients were recruited in accordance  
35 with local ethics approval from Birmingham University and Tayside ethics committees.  $[\text{Ca}^{2+}]_i$   
36 responses and  $V_m$  of individual cells were examined by fluorescence imaging and whole-cell current  
37 clamp.

38 **Main results and the role of chance:** P4-induced  $[\text{Ca}^{2+}]_i$  oscillations originated in the flagellum,  
39 spreading to the neck and head (latency of 1-2 s).  $\text{K}^+$ -ionophore valinomycin (1  $\mu\text{M}$ ) was used to  
40 investigate the role of membrane potential ( $V_m$ ). Direct assessment by whole-cell current-clamp  
41 confirmed that  $V_m$  in valinomycin-exposed cells was determined primarily by  $\text{K}^+$  equilibrium  
42 potential ( $E_K$ ) and was rapidly 'reset' upon manipulation of  $[\text{K}^+]_o$ . Pretreatment of sperm with  
43 valinomycin ( $[\text{K}^+]_o=5.4 \text{ mM}$ ) had no effect on the P4-induced  $[\text{Ca}^{2+}]$  transient ( $P=0.95$ ; 8  
44 experiments), but application of valinomycin to P4-pretreated sperm suppressed activity in 82% of  
45 oscillating cells ( $n=257$ ;  $P=5*10^{-55}$  compared to control) and significantly reduced both amplitude  
46 and frequency of persisting oscillations ( $p=0.0001$ ). Upon valinomycin washout oscillations re-started  
47 in most cells. When valinomycin was applied in saline with elevated  $[\text{K}^+]$  the inhibitory effect of

48 valinomycin was reduced and was dependent on  $E_K$  ( $P=10^{-25}$ ). Amplitude and frequency of  $[Ca^{2+}]_i$   
49 oscillations that persisted in the presence of valinomycin showed similar sensitivity to  $E_K$  ( $P<0.01$ ).  
50 The CatSper inhibitor RU1968 (4.8 and 11  $\mu$ M) caused immediate and reversible arrest of activity in  
51 36% and 96% of oscillating cells respectively ( $P<10^{-10}$ ). 300  $\mu$ M quinidine which blocks the sperm  $K^+$   
52 current ( $K_{sper}$ ) completely inhibited  $[Ca^{2+}]_i$  oscillations.

53 **Large scale data:** n/a

54 **Limitations, reasons for caution:** This was an in-vitro study and caution must be taken when  
55 extrapolating these results to in vivo regulation of sperm.

56 **Wider implications of the findings:**  $[Ca^{2+}]_i$  oscillations in human sperm are functionally important  
57 and their absence is associated with failed fertilisation at IVF. The data reported here provide new  
58 understanding of the mechanisms that underlie the generation (or failure) and regulation of these  
59 oscillations.

60 **Study funding/competing interest(s):** ET was in receipt of a postgraduate scholarship from the  
61 CAPES Foundation (Ministry of Education, Brazil). The authors have no conflicts of interest.

62

## 63 **Introduction**

64  $\text{Ca}^{2+}$ -signalling plays an essential role in the regulation of sperm cell function. Key activities,  
65 including motility, acrosome reaction and capacitation (acquisition of fertilising ability) are regulated  
66 through intracellular calcium concentration ( $[\text{Ca}^{2+}]_i$ ) and can be modified by artificial manipulation of  
67  $\text{Ca}^{2+}$ -signalling processes (Darszon, et al., 2011, Publicover, et al., 2007, Suarez, 2008). In most  
68 animal phyla the primary plasma membrane  $\text{Ca}^{2+}$  channel of sperm is CatSper (Cai and Clapham,  
69 2008, Ren, et al., 2001), which can be activated upon encountering a stimulus, generating an  
70 immediate increase in cytoplasmic  $[\text{Ca}^{2+}]_i$  and a consequent change in the activity of the cell. For  
71 instance, in sea urchin sperm, activation of CatSper induced by binding of chemoattractant molecules  
72 to their receptors (Seifert, et al., 2015) induces a transient elevation of  $[\text{Ca}^{2+}]_i$  that causes the sperm to  
73 re-orientate its path up the chemoattractant gradient (Guerrero, et al., 2010, Kaupp, et al., 2008).  
74 Similarly, in human sperm activation of CatSper channels by progesterone (P4) results in a  $[\text{Ca}^{2+}]_i$   
75 transient which induces a brief, but marked, modification of flagellar beating (Bedu-Addo, et al.,  
76 2007, Schiffer, et al., 2014, Smith, et al., 2013).

77 As well as phasic  $\text{Ca}^{2+}$  signals that are induced upon presentation of a stimulus, human sperm  
78 generate repetitive  $[\text{Ca}^{2+}]_i$  spikes or oscillations, either during prolonged exposure to a stimulus or  
79 even 'spontaneously', in the absence of any applied stimulus (Harper, et al., 2004, Mata-Martinez, et  
80 al., 2018). The functional significance of these signals is not clear. Initial observations on loosely  
81 immobilised cells exposed to a prolonged P4 stimulus showed that each  $[\text{Ca}^{2+}]_i$  spike or oscillation  
82 peak was associated with a temporary increase in the amplitude of flagellar excursion (Harper, et al.,  
83 2004), suggesting that these signals may be involved in regulation of flagellar beat mode. More  
84 recently it has been shown that occurrence of acrosome reaction is suppressed in cells displaying  
85 spontaneous  $[\text{Ca}^{2+}]_i$  oscillations (Sanchez-Cardenas, et al., 2014) and that ability to undergo acrosome  
86 reaction can be restored by inhibition of these  $[\text{Ca}^{2+}]_i$  signals (Mata-Martinez et al, 2018). The  
87 occurrence of samples that completely failed to generate  $[\text{Ca}^{2+}]_i$  oscillations in response to P4 was  
88 significantly higher in men who failed to fertilise at IVF compared to samples from donors and  
89 patients who fertilised (Kelly, et al., 2018).

90 Repetitive  $[Ca^{2+}]_i$  activity in somatic cells is typically generated by mobilisation of  $Ca^{2+}$  stored in  
91 intracellular organelles, such as the endoplasmic reticulum. Upon stimulation the storage organelles  
92 are cyclically emptied (by activation of  $Ca^{2+}$  channels) and refilled (by activity of  $Ca^{2+}$ -ATPases)  
93 resulting in an oscillatory  $Ca^{2+}$  signal (Berridge, et al., 1988, Berridge, et al., 2003). Sperm cells  
94 appear to possess at least two  $Ca^{2+}$  storage organelles which have  $Ca^{2+}$  channels and  $Ca^{2+}$ -ATPases  
95 similar to those in somatic cells (Correia, et al., 2015, Costello, et al., 2009) and pharmacological  
96 studies indicate that these stores are involved in the generation of oscillatory  $Ca^{2+}$  signals in human  
97 sperm (Harper, et al., 2004, Mata-Martinez, et al., 2018). However, in both excitable and non-  
98 excitable cells, oscillation of  $[Ca^{2+}]_i$  can also occur due to interaction between voltage-sensitive  $Ca^{2+}$ -  
99 channels and  $Ca^{2+}$  sensitive  $K^+$  channels, resulting in cyclic changes in membrane potential ( $V_m$ ) and  
100 consequent bursts of  $Ca^{2+}$ -influx (e.g. Gorman and Thomas, 1978, Lopez, et al., 1995, Schlegel, et al.,  
101 1987). Significantly, though stored  $Ca^{2+}$  is implicated in the mechanism underlying  $Ca^{2+}$  oscillations  
102 in human sperm, extracellular  $Ca^{2+}$  is required for their generation and/or persistence (Harper, et al.,  
103 2004, Mata-Martinez, et al., 2018) suggesting that regulation of membrane  $Ca^{2+}$  permeability is  
104 involved in generating or shaping repetitive  $[Ca^{2+}]_i$  activity. We have therefore investigated the  
105 initiation of  $[Ca^{2+}]_i$  oscillations in human sperm and the potential involvement of CatSper and  
106 regulation by  $V_m$ .

107



## 108 **Methods**

109 *Materials* All chemicals were obtained from Sigma-Aldrich (Poole, UK) except fluo4-AM  
110 (acetoxymethylester), which was from Thermo Fisher Scientific, UK. Fluo4-AM was prepared in  
111 dimethylsulphoxide (DMSO) containing 20% Pluronic F-127 (Thermo Fisher). P4 and RU1968 were  
112 dissolved in DMSO at 10 mM and diluted in sEBBS prior to use. Quinidine was dissolved in DMSO at  
113 100 mM and diluted in sEBBS prior to use. RU1968 was a kind gift of Dr Timo Strünker, Centre of  
114 Reproductive Medicine and Andrology, Münster, Germany,

115

116 *Salines* The standard incubation medium used in this study was supplemented Earle's balanced salt  
117 solution (sEBSS), containing NaCl (90 mM), KCl (5.4 mM), CaCl<sub>2</sub> (1.8 mM), MgCl<sub>2</sub> (1 mM),  
118 glucose (5.5 mM), NaHCO<sub>3</sub> (25 mM), Na pyruvate (2.5 mM), Na lactate (19 mM), MgSO<sub>4</sub> (0.81  
119 mM), HEPES (15 mM) and 0.3% bovine serum albumin (BSA). The pH was adjusted to 7.4 with  
120 NaOH and osmolarity was then adjusted to 291-294 mOsm as necessary by adding NaCl. Salines with  
121 increased [K<sup>+</sup>] were made by isotonic replacement of NaCl with KCl. 'Ca<sup>2+</sup>-free' saline was made by  
122 omission of CaCl<sub>2</sub> ([Ca<sup>2+</sup>]<sub>i</sub> < 5 μM; Harper, et al., 2004) and in EGTA-buffered saline CaCl<sub>2</sub> was  
123 omitted and 2 mM EGTA was added (calculated [Ca<sup>2+</sup>]<sub>i</sub> = 2.6 \* 10<sup>-10</sup> M; Maxchelator (Webmaxc  
124 standard); UC, Davis). Intracellular (pipette) solution for current clamp recordings contained NaCl  
125 (10 mM), KCl (18 mM), K gluconate (92 mM), MgCl<sub>2</sub> (0.5 mM), CaCl<sub>2</sub> (0.6 mM), EGTA (1 mM),  
126 HEPES (10 mM), pH adjusted to 7.4 using KOH, which brought [K<sup>+</sup>]<sub>i</sub> to 114 mM and [Ca<sup>2+</sup>]<sub>i</sub> to 0.11  
127 μM (Webmaxc standard).

128

129 *Selection and preparation of spermatozoa* Written consent was obtained from donors in accordance  
130 with the Human Fertilisation and Embryology Authority (HFEA) Code of Practice (version 8) under  
131 local ethical approval (University of Birmingham (ERN 07-009 and ERN-12-0570) and Tayside  
132 Committee of Medical Research Ethics (13/ES/0091)). **Semen samples were from donors with normal**  
133 **sperm concentration and motility (measured parameters for all samples exceeded the lower reference**  
134 **limits; WHO 2010; table S1).** Samples were obtained by masturbation after 2-3 days sexual

135 abstinence. After liquefaction (30 min), sperm were swum up into sEBSS (60 min), adjusted to a  
136 maximum of  $\approx 6$  million/ml and left to capacitate ( $36^{\circ}\text{C}$ , 5.5%  $\text{CO}_2$ ) for 5 hours.

### 137 Current Clamp

138 To monitor membrane  $V_m$  directly, electrophysiological recordings were conducted on sperm, bathed  
139 in sEBSS, using whole-cell, zero current clamp. Recording pipettes were filled with standard  
140 intracellular solution and gigaseals were achieved by carefully manoeuvring the tip of the pipette onto  
141 the neck region of the sperm and applying gentle suction. This was followed by another brief suction  
142 to achieve the whole-cell configuration. Data were acquired at 5 KHz and low pass filtered at 3 KHz  
143 using an Axopatch 200B (Molecular Devices). Data presented are adjusted for liquid junction  
144 potential.

145 Collection and analysis of imaging data. Imaging was carried out essentially as described in (Nash, et  
146 al., 2010). Briefly, after adjusting cell concentration to  $1.5 \times 10^6$  million/ml the cell suspension was  
147 divided into aliquots of 200  $\mu\text{L}$  and incubated with fluo4-AM (5  $\mu\text{M}$ ) for 30 min ( $36^{\circ}\text{C}$ , 5.5%  $\text{CO}_2$ ).  
148 Cells were then transferred to a perfusable imaging chamber, the base of which was a coverslip coated  
149 with 0.001% poly-D-lysine and incubated for an additional 5 minutes to allow cells to settle. The  
150 chamber was installed on the stage of an inverted fluorescence microscope (Nikon TE300) and  
151 perfused with sEBSS to remove unattached cells and excess dye. All experiments were performed at  
152  $25^{\circ}\text{C}$  in a continuous flow of sEBSS, with a perfusion rate of 0.6 ml/minute. Fluorescence excitation  
153 was at 470 nm (OptoLED, Cairn, UK) and emission at 520 nm. Images were captured at 0.2 Hz  
154 except for localisation of signal initiation (2.5 Hz) using a 40 $\times$  or 60 $\times$  oil-immersion objective and an  
155 Andor Ixon 897 EMCCD camera controlled by iQ3 software (Andor Technology, Belfast). Stimuli  
156 were applied to the cells by inclusion in the perfusing medium. In experiments where valinomycin  
157 exposure was combined with modified  $[\text{K}^+]_o$  the cells were maintained in standard sEBSS except  
158 during the period of exposure to valinomycin.

159 Analysis of images and background correction was done using iQ3 software. Regions of interest were  
160 drawn around the required area(s) and the background subtracted. Average intensity was obtained for  
161 each area. Analysed and plotted data refer to the signal obtained from the posterior head/neck except

162 where more detailed regional analysis is described. For comparison of fluorescence in multiple  
163 regions within the sperm, cells with an adequately-immobilised flagellum were selected for analysis  
164 in order that fluorescence could be recorded from regions of interest in the flagellum as well as from  
165 the sperm neck and post-acrosomal head. Raw intensity values were imported into Microsoft Excel  
166 and normalized by calculating percentage change in fluorescence ( $\Delta F$ ) using the equation:

$$167 \quad \Delta F = [(F - F_{rest})/F_{rest}] \times 100\%$$

168 where  $\Delta F$  is the percentage change in fluorescence intensity at time t, F is fluorescence intensity at  
169 time t and  $F_{rest}$  is the mean of  $\geq 10$  determinations of F during the control period before application of  
170 P4.

171 Repetitive  $[Ca^{2+}]_i$  activity (oscillations) induced by 3  $\mu M$  P4 stimulation was analysed for amplitude  
172 and frequency. Oscillation (and P4-induced transient) amplitudes were calculated, for each event, as  
173 the increment in  $\Delta F$  (calculated as the difference between the  $\Delta F$  values at the signal peak and  
174 immediately before onset of the signal). For each cell mean amplitude for the experimental  
175 (treatment) period was then calculated and either normalised to the equivalent mean for the preceding  
176 control period or expressed a % of the amplitude of the initial P4-induced transient. Background  
177  $[Ca^{2+}]_i$  noise or 'ripples' with amplitude  $< 20\%$  of the amplitude of the preceding P4-induced transient  
178 peak were not considered oscillations. Latency of  $[Ca^{2+}]_i$  signals in the sperm head and neck  
179 (compared to the proximal flagellum) was estimated directly from the traces by identifying the start of  
180 the rising phase of the fluorescence signal (inflexion in the fluorescence trace) in each of the different  
181 regions. Oscillation frequency was estimated by counting the number of  $[Ca^{2+}]_i$  spikes and dividing by  
182 time. Oscillation duration was assessed by taking the period between initiation and complete decay of  
183 the  $[Ca^{2+}]_i$  signal.

184 Calculation of effective dose of RU1968. We have previously reported that compounds applied by  
185 superfusion may be present in the imaging chamber at concentrations significantly lower than that  
186 applied to the perfusion inflow (Brown, et al., 2017). In pilot experiments, the potency of RU1968  
187 was lower than previously reported (Rennhack, et al., 2018). We therefore carried out parallel

188 experiments to compare the efficacy of RU1968 (1, 10, 20 and 30  $\mu\text{M}$ ), when applied by superfusion  
189 of the imaging chamber and when used in a static incubation chamber (multiwell plate; Achikanu, et  
190 al., 2018), in blocking the  $[\text{Ca}^{2+}]_i$  transient induced by 3  $\mu\text{M}$  P4. Data obtained with each method were  
191 fitted with a four parameter logistic regression model ( $Y = \text{min} + (\text{max}-\text{min})/1 + (X/\text{IC}_{50})^{\text{Hill}}$   
192 coefficient) using <https://mycurvefit.com/>.

193           When RU1968 was applied by addition to a static chamber the calculated  $\text{IC}_{50}$  was 6.9  $\mu\text{M}$ ,  
194 similar to the previously reported value of 5.5  $\mu\text{M}$  (Rennhack, et al., 2018). However, when applied  
195 by superfusion  $\text{IC}_{50}$  was 18.4  $\mu\text{M}$  (fig S1). From the fitted curves we estimate that effective  
196 concentrations achieved by adding 10 and 30  $\mu\text{M}$  RU1968 to the perfusing medium were 4.8 and 11.0  
197  $\mu\text{M}$  respectively (fig S1).

198

199 Statistics. Data were assessed for normality using the Anderson-Darling method and tested  
200 accordingly. Chi-square test was used for categorical variables (with adjustment for multiple testing  
201 as appropriate). t-test (paired or independent), Mann-Whitney or Wilcoxon test, with adjustment for  
202 multiple testing as appropriate, were used for continuous variables. ANOVA or Kruskal-Wallis test  
203 was used for comparing multiple groups.

204 **Results**

205 Following stimulation with 3  $\mu\text{M}$  P4, repetitive  $[\text{Ca}^{2+}]_i$  activity (repetitive spiking or oscillatory  
206 activity) was observed in a sub-population of human sperm, occurrence varying between samples (10-  
207 50% of cells). Mean amplitude was  $53.2 \pm 1.3\%$  of the preceding P4-induced transient (310 oscillations  
208 in 101 cells) and mean frequency was  $0.46 \pm 0.02$  cycles.min<sup>-1</sup> (101 cells).

209  *$[\text{Ca}^{2+}]_i$  oscillations initiate in the flagellum.* In order to investigate how repetitive  $\text{Ca}^{2+}$  signals are  
210 generated, we first assessed their point of origin and spread within the sperm cell. Images were  
211 captured at 2.5 Hz and regions of interest were analysed in the head, neck region/midpiece and in the  
212 principal piece of the flagellum at points approximately 1/3 ( $\approx 15$   $\mu\text{M}$ ; proximal) and 2/3 ( $\approx 30$   $\mu\text{m}$ ,  
213 distal) of the distance from midpiece to tip. Examination of traces obtained from the different regions  
214 of interest showed that elevation of  $[\text{Ca}^{2+}]_i$  consistently initiated in the principal piece. Start time of  
215 the  $[\text{Ca}^{2+}]_i$  signal in the proximal and distal flagellum were similar ( $P > 0.1$ ) but the signals in the neck  
216 and head occurred with a latency of  $1.47 \pm 0.14$  and  $2.21 \pm 0.20$  s respectively, compared to the  
217 proximal flagellum ( $P < 0.001$ ; 21 cells; Wilcoxon; fig 1a,b, video 1, fig S2a). Latency of signal spread  
218 from the principal piece to the head showed no dependence on the order of occurrence in the  
219 oscillation series (first 4 oscillations,  $P > 0.8$ ; Kruskal-Wallis with post hoc comparison). For  
220 comparison, we also examined the preceding P4-induced  $[\text{Ca}^{2+}]_i$  transient. The transient initiated in  
221 the principal piece with latencies to the neck and head of  $1.40 \pm 0.34$  s ( $n=18$  cells;  $p > 0.8$  compared to  
222 oscillations) and  $2.30 \pm 0.35$  s respectively ( $n=21$  cells;  $P > 0.8$  compared to oscillations; fig 1b, video  
223 2; fig S2a).

224 Signal amplitude (increment in  $\Delta F$  calculated as the difference between the  $\Delta F$  values at the signal  
225 peak and immediately before onset of the signal) was also assessed at the four regions of interest.  
226 Fluorescence increments in the head and neck were significantly greater than in the flagellum  
227 ( $P = 2.2 \times 10^{-5}$ ; ANOVA with Tukey post hoc comparison; fig 1c). Equivalent analysis of the amplitude  
228 of the initial P4-induced  $[\text{Ca}^{2+}]_i$  transient showed that though the mean amplitude was slightly larger

229 at the head and neck than in the flagellum, there was no significant difference between regions within  
230 the cell ( $P=0.67$ , ANOVA; fig 1d)

231 Since  $[Ca^{2+}]_i$  oscillations originate in the principal piece of the flagellum, the most likely source for  
232 this initial  $Ca^{2+}$  increase is influx at the plasma membrane. In previous studies we showed that  $[Ca^{2+}]_i$   
233 oscillations are rapidly terminated in saline with no added  $Ca^{2+}$  and buffered with 2 mM EGTA,  
234 suggesting that mobilisation of stored  $Ca^{2+}$  cannot sustain oscillations in the absence of  $Ca^{2+}$  influx.  
235 However, when  $Ca^{2+}$  was simply omitted from the saline (' $Ca^{2+}$  free' -  $[Ca^{2+}] < 5 \mu M$ ), oscillations  
236 persisted and were often enlarged, primarily because the troughs between peaks approached more  
237 nearly to resting  $[Ca^{2+}]_i$  (Harper, et al., 2004). Since EGTA buffered saline may cause rapid depletion  
238 of stored  $Ca^{2+}$  (Bedu-Addo et al., 2007), the inhibitory effect of EGTA-buffered saline on oscillations  
239 cannot be considered proof that  $Ca^{2+}$ -influx is essential, leaving the possibility that repeated  
240 mobilisation of stored  $Ca^{2+}$  (and consequent oscillation of  $[Ca^{2+}]_i$ ) can occur under conditions of  
241 greatly reduced  $Ca^{2+}$  influx. To investigate this further we observed the effect on oscillations of  
242 prolonged superfusion with ' $Ca^{2+}$ -free' saline. As described previously (Harper, et al., 2004), after a  
243 brief hiatus, oscillations persisted in cells superfused with ' $Ca^{2+}$  free' saline. However, after a further  
244 5-15 min both rise and decay time of oscillations slowed and  $[Ca^{2+}]_i$  eventually settled at a level close  
245 to or below the initial resting value (fig 1e blue shading; mean time to arrest= $12.3 \pm 0.5$  min; max  
246 = $22.7$  min;  $n=51$  cells from 3 experiments). Subsequent addition of EGTA caused an immediate fall  
247 in  $[Ca^{2+}]_i$  to very low levels (fluo4 fluorescence was 30-80% below the initial resting value; fig 1e  
248 grey shading). As reported previously,  $[Ca^{2+}]_i$  did not recover when EGTA was removed (Bedu-Addo  
249 et al., 2007, Harper, et al., 2004) but upon return to standard sEBSS  $[Ca^{2+}]_i$  immediately rose to a  
250 plateau level that exceeded the amplitude of the P4-induced transient (20-200% greater).

251 *Hyperpolarisation of  $V_m$  inhibits  $[Ca^{2+}]_i$  oscillations.* Since  $[Ca^{2+}]_i$  oscillations originate in the  
252 flagellum, where  $Ca^{2+}$  signals will be generated by influx at the plasma membrane, we investigated  
253 the possible involvement of  $V_m$  in regulating membrane  $Ca^{2+}$  channels, by using the  $K^+$  ionophore  
254 valinomycin (1  $\mu M$ ) to 'clamp' the membrane at  $E_K$  ( $\approx -78$  mV assuming  $[K^+]_i=120$  mM).  
255 Valinomycin uncouples mitochondria (e.g. Felber and Brand, 1982, Salvioli, et al., 2000) and can

256 cause a small increase in  $[Ca^{2+}]_i$  in human sperm, but we have shown previously that mitochondrial  
257 uncouplers do not inhibit generation of  $[Ca^{2+}]_i$  oscillations in human sperm (Harper, et al., 2004,  
258 Machado-Oliveira, et al., 2008). We first assessed the efficacy of valinomycin by directly observing  
259  $V_m$  of cells held in whole cell current clamp. In cells bathed in standard sEBSS ( $[K^+]=5.4$  mM), mean  
260  $V_m$  of dialysed cells (1 min after breakthrough into whole cell recording mode) was  $-42.7 \pm 3.7$  mV  
261 ( $n=6$ ). Upon exposure to valinomycin,  $V_m$  rapidly hyperpolarised (fig 2a), settling at  $-72.5 \pm 1.6$  mV  
262 within  $\approx 2$  min (fig 2). Subsequent change to valinomycin saline containing 100 mM  $K^+$  induced a  
263 rapid (within 1 min) shift to a stable value of  $-9.0 \pm 1.5$  mV, which could be reversed by return to  
264 standard saline (fig 2a). These values fall close to those for  $E_K$  predicted by the Nernst equation ( $-76.8$   
265 mV and  $-3.3$  mV) for the known intra- and extracellular  $K^+$  concentrations (fig S3).

266 When cells bathed in standard (5.4 mM  $K^+$ ) saline were exposed to valinomycin we saw a small,  
267 sustained increase in  $[Ca^{2+}]_i$ , as observed previously (Fraire-Zamora and Gonzalez-Martinez, 2004,  
268 Linares-Hernandez, et al., 1998). Subsequent application of 3  $\mu$ M P4 induced a  $[Ca^{2+}]_i$  transient  
269 similar to that observed in parallel controls without valinomycin pretreatment (fig 3a,b;  $p=0.95$   $n=8$ ;  
270 paired t), indicating that this saturating dose of P4 can effectively gate CatSper in cells clamped to  $\approx$ -  
271 75 mV. However, following the initial transient, the occurrence of  $[Ca^{2+}]_i$  oscillations was negligible  
272 until washout of valinomycin, upon which many cells became active, indicating that oscillations,  
273 unlike the initial transient, may be inhibited by hyperpolarisation of  $V_m$  (fig 3c). To further assess this  
274 effect we reversed the order of treatment, first stimulating cells with P4 to induce an 'oscillating' sub-  
275 population (activity with amplitude  $\geq 20\%$  of the preceding P4-induced transient), then exposing the  
276 cells to valinomycin in the continued presence of P4. Superfusion with 1  $\mu$ M valinomycin rapidly  
277 suppressed activity (fig 4a, video 3, fig S2b), oscillations persisting in only 18.3% of the oscillating  
278 sub-population (47/257 cells in 16 experiments) after hyperpolarisation of  $V_m$ , compared to 99%  
279 (147/149) in control experiments (fig 5a;  $p=5 \times 10^{-55}$ ; chi square). In 7 experiments the valinomycin  
280 was washed off after 15 min exposure and recording was continued for a further 15 min. Of 94 cells  
281 where valinomycin caused arrest of oscillations, 62 (66%) restarted, activity appearing within  $\approx 5$  min  
282 of valinomycin washout (fig 4a, video 3, fig S2b). In those cells where activity persisted in the

283 presence of valinomycin, both the amplitude and frequency of the  $[Ca^{2+}]_i$  signals were reduced (fig  
284 4a). To quantify this effect we selected 22 cells (from 3 experiments) and analysed the characteristics  
285 of the oscillations that persisted in the presence of valinomycin. Upon application of valinomycin both  
286 amplitude and frequency of the persisting oscillations were reduced to approximately one third of  
287 their values in the preceding control period ( $P \leq 0.0001$ ; Mann-Whitney and paired t respectively; fig  
288 5b,c).

289 Effect of valinomycin treatment is dependent on  $E_K$ . To, assess the importance of hyperpolarisation in  
290 the observed inhibition of  $[Ca^{2+}]_i$  oscillations by valinomycin, we repeated the experiments, applying  
291 valinomycin in the presence of 25 mM  $K^+$  ( $E_K = -39.5$  mV with  $[K^+]_i = 120$  mM; similar to the  
292 measured resting potential) and 100 mM  $K^+$  (conditions which should fully depolarise  $V_m$ ;  $E_K = -4.6$   
293 mV with  $[K^+]_i = 120$  mM). When co-applied with 25 mM  $K^+$  the inhibition by valinomycin was still  
294 observed (video 4, fig S2c) but the effect of significantly ameliorated, almost half of oscillating cells  
295 (58/117 in 3 experiments) remaining active (figs 4b, 5a). When valinomycin was co-applied with 100  
296 mM  $K^+$  there was a more marked increase in underlying  $[Ca^{2+}]_i$  (compare figs 4a and 4c) and the  
297 inhibitory effect on  $[Ca^{2+}]_i$  oscillations was further reduced, activity persisting in over 75% (86/114)  
298 of oscillating cells (figs 4c, 5a, video 5, fig S2d). Comparison across the three conditions confirmed  
299 that the efficacy of valinomycin in suppressing activity was highly dependent on  $[K^+]_o$  ( $P = 10^{-25}$ ; chi-  
300 square).

301 Examination of the characteristics of oscillations in those cells where spontaneous activity persisted in  
302 the presence of valinomycin showed that the effects of treatment on amplitude and (more particularly)  
303 frequency were similarly dependent on the extracellular  $K^+$  concentration. As in standard sEBSS,  
304 exposure to valinomycin reduced both the amplitude and frequency of oscillations, but these effects  
305 were dependent on  $[K^+]_o$ , being ameliorated as  $E_K$  was shifted to more positive values (fig 4; fig 5b,c;  
306  $P = 0.003$  (Kuskal-Wallis) and  $P = 10^{-6}$  (ANOVA) for amplitude and frequency respectively). When  
307 valinomycin was washed out (combined with a return to standard sEBSS) spontaneous activity was  
308 able to recover. In cells exposed to valinomycin in 25 mM and 100 mM  $K^+$  saline, oscillations  
309 restarted in 45/59 (76%) and 12/28 (43%) of previously oscillating cells respectively. Following



310 valinomycin/100 mM K<sup>+</sup> treatment the delay before activity resumed was noticeably longer  
311 (typically  $\geq 15$  min; fig 4c).

312

313 *Blockade of CatSper reversibly inhibits  $[Ca^{2+}]_i$  oscillations.* CatSper, the primary Ca<sup>2+</sup> channel of  
314 human sperm, is voltage sensitive and is localised to the sperm flagellum (Lishko, et al., 2011). To  
315 assess the involvement of CatSper in generation of oscillations, we tested the effect of RU1968, a  
316 ‘specific’ blocker which does not affect pHi and has limited effects on sperm K<sup>+</sup> conductance  
317 (Rennhack, et al., 2018). Sperm were first exposed to P4 to establish oscillations in a sub-population  
318 of cells, then RU1968 was applied, in the continued presence of P4.

319 At an estimated concentration of 11  $\mu$ M (see methods), spontaneous activity was rapidly and  
320 completely inhibited in the great majority of oscillating cells, only 6.9% of the oscillating cells  
321 remaining active (4/58 cells in 3 experiments; fig.6a, 7a, video 6, fig S2e), compared to 98.9% (88/89)  
322 in parallel controls exposed to 0.3% DMSO ( $p=10^{-29}$ ; Chi-square). It was noticeable that, unlike the  
323 effect of valinomycin, background  $[Ca^{2+}]_i$  noise or ‘ripples’ (amplitude  $<20\%$ ) were also largely  
324 suppressed (compare figs 4a and 6a). Each of the 4 cells in which activity persisted generated a single  
325 transient during the 10 min period of exposure to RU1968. Amplitude of these  $[Ca^{2+}]_i$  signals varied  
326 from 20-100% of those recorded during the preceding control period. Upon washout of the drug  
327 (exposure time=10 min), spontaneous activity recovered in 80% (43/54) of the cells where treatment  
328 had caused arrest of activity.

329 Exposure to an estimated concentration of 4.8  $\mu$ M RU1968 caused a transient increase in  $[Ca^{2+}]_i$  in all  
330 cells, which varied greatly in amplitude and decayed within 3-5 min (fig 6b, video , fig S2f; compare  
331 to 11  $\mu$ M [figs 6a, S2e] where immediate suppression of activity occurs). Oscillations persisted in  
332 64.3% of the cells that were previously active (83/129 cells, 3 experiments; fig 6b, 7a;  $P=8*10^{-14}$   
333 compared to 11  $\mu$ M) whereas in parallel control experiments oscillations persisted in 98.3% of cells  
334 (59/60 cells;  $p=10^{-6}$ ; Chi-square). In those cells that continued to generate spontaneous activity the  
335 characteristics of the  $[Ca^{2+}]_i$  signals were clearly modified (fig 6b, video 7, fig S2f). The frequency of

336 persisting oscillations was reduced by almost 50% (fig 7b;  $P < 10^{-16}$ ; Mann-Whitney) and both the  
337 amplitude of oscillations (fig 7c) and their duration (fig 7d) were significantly increased compared to  
338 the preceding control period ( $P = 1.5 \times 10^{-5}$ , paired t and  $P < 10^{-16}$ , Mann-Whitney, respectively). When  
339 RU1968 was washed out of the recording chamber spontaneous activity recovered in 72% (33/46) of  
340 the cells where oscillations had been inhibited ( $P = 0.73$  compared to 11  $\mu\text{M}$ ; chi square). In  
341 approximately half (20/38) of those cells where P4 treatment had failed to induce significant  
342 oscillations (defined as  $\geq 20\%$  of the preceding P4-induced transient; see methods), the transient  
343  $[\text{Ca}^{2+}]_i$  increase that occurred upon application of 4.8  $\mu\text{M}$  RU1968 was followed by second large,  
344 slow oscillation (fig S4). Repetitive activity persisted after washout of RU1968 in 8 of these cells.

345 *The KSper blocker quinidine inhibits  $[\text{Ca}^{2+}]_i$  oscillations.* Quinidine (300  $\mu\text{M}$ ) blocked KSper  
346 currents in human sperm by  $\approx 90\%$  (Mansell, et al., 2014) and potently blocks mouse Slo3 (KSper)  
347 channels (Tang et al, 2010). Application of 300  $\mu\text{M}$  quinidine to cells in which oscillations had  
348 previously been established by exposure to P4 resulted in complete block of  $[\text{Ca}^{2+}]_i$  activity (36/36  
349 cells; fig 6c;  $P = 1.7 \times 10^{-30}$  compared to control, chi-square). Similarly to treatment with RU1968,  
350  $[\text{Ca}^{2+}]_i$  noise or ‘ripples’ (amplitude  $< 20\%$ ) were also suppressed in most cells (fig 6c). Upon washout  
351 (exposure time=10 min) there was an immediate  $[\text{Ca}^{2+}]_i$  spike, even in those cells in which oscillations  
352 were not previously observed, but restart of oscillations occurred in only 6/36 cells (16.7%),  
353 significantly lower than the responses seen under any other of the treatments tested ( $P < 0.05$ ; chi  
354 square).

355

356

## 357 Discussion

358 We and others have reported the occurrence of repetitive  $[Ca^{2+}]_i$  elevations, in human sperm, that  
359 contribute to regulation of key sperm functions (Bedu-Addo et al., 2007, Harper, et al., 2004,  
360 Machado-Oliveira, et al., 2008, Mata-Martinez, et al., 2018, Sanchez-Cardenas, et al., 2014). Here we  
361 have further investigated the mechanisms by which these signals are generated.

362 Oscillations originate in the flagellum. Consistent with previous reports (Servin-Vences, et al., 2012;  
363 Alasmari, et al., 2013), the initial P4-induced  $[Ca^{2+}]_i$  transient initiated in the flagellar principal piece.  
364 Oscillations behaved similarly, propagating from the flagellum to the head/neck region with kinetics  
365 similar to those of the initial transient. Oscillation amplitude measured at the sperm head/neck, was  
366 significantly greater than at the flagellum. This observation is consistent with mobilisation of a  
367 secondary  $Ca^{2+}$  source in this region (Bedu-Addo et al., 2007; Olson, et al., 2010, Publicover, 2017).  
368 However, this must be interpreted cautiously. A non-ratiometric dye was used in this study and  
369 apparent regional variation in the normalised responses might be due to other factors, such as  
370 differences in resting  $[Ca^{2+}]_i$  between flagellum and sperm head.

371 Oscillations are dependent on  $V_m$ . Manipulation of  $V_m$  with valinomycin, (fig 2), had no effect on  
372 the P4-induced  $[Ca^{2+}]_i$  transient, possibly because of the saturating concentration of P4 used in this  
373 study. In contrast, oscillations were strongly suppressed by valinomycin-induced hyperpolarisation.  
374 This inhibition was ameliorated when  $V_m$  was set to more +ve potentials. If fluctuation of  $V_m$  plays a  
375 role in P4-induced  $[Ca^{2+}]_i$  oscillation (see below), limited cyclic regulation of  $V_m$  must persist in  
376 these cells, despite the presence of valinomycin. We conclude that initiation of oscillations in the  
377 flagellar principal piece is regulated by or sensitive to  $V_m$ .

378 Blockade of CatSper and K<sub>Sper</sub> inhibits oscillations. Since  $[Ca^{2+}]_i$  oscillations require extracellular  
379  $Ca^{2+}$  (fig. 1e) we investigated the importance of CatSper. The CatSper blocker RU1968 ( $IC_{50} \approx 5 \mu M$ )  
380 dose-dependently suppressed  $[Ca^{2+}]_i$  oscillations. Though the drug also inhibits Slo3, this action is 15-  
381 fold less potent than CatSper block (Rennhack, et al., 2018). The effects of RU1968 reported here  
382 (particularly the lower dose estimated at 4.8  $\mu M$ ) will reflect primarily its action on CatSper and we

383 therefore conclude that initiation of oscillations in the flagellum involves CatSper-mediated  $\text{Ca}^{2+}$ -  
384 influx. Intriguingly, where oscillations persisted in the presence of RU1968, their frequency was  
385 reduced but amplitude and duration were significantly increased. This may reflect resetting of the  
386 'oscillator' in the flagellum due to reduced currents through CatSper, or might even be oscillatory  
387 behaviour of  $\text{Ca}^{2+}$  stores persisting after inhibition of  $\text{Ca}^{2+}$  influx.

388 Quinidine (300  $\mu\text{M}$ ), which blocks human KSper (Brenker, et al., 2014; Mansell, et al., 2014), was  
389 strikingly effective in arresting  $[\text{Ca}^{2+}]_i$  oscillations. However, in addition to its action on KSper, 300  
390  $\mu\text{M}$  quinidine blocks CatSper currents (Zeng et al., 2011; Mansell, et al., 2014) an effect that might  
391 underlie our observations. However, it is noteworthy that recovery of oscillations following washout  
392 of RU1968 was rapid (80% of silenced cells recovered) whereas no recovery was seen with quinidine  
393 (compare figs 6a and 6c). In whole cell patch clamp recordings the effects of quinidine on CatSper  
394 currents washed out rapidly (30 s) whereas KSper recovered more slowly (3-4 min; Mansell, et al.,  
395 2014), which might underlie this observation.

396 Generation of  $[\text{Ca}^{2+}]_i$  oscillations in human sperm. The data presented here do not allow us to  
397 develop a clear model for the mechanism underlying the generation of repetitive  $[\text{Ca}^{2+}]_i$  activity in the  
398 flagellum of P4-stimulated human sperm. However, since (i) their generation is dependent on  $V_m$  and  
399 requires activity of CatSper and probably KSper, (ii) CatSper opening is increased by depolarisation  
400 of  $V_m$ , (iii) KSper, which regulates  $V_m$ , is stimulated by elevated  $[\text{Ca}^{2+}]_i$  (Brenker, et al., 2014,  
401 Brown, et al., 2016; Mannowetz, et al., 2013), oscillations could involve a feedback loop in which  
402  $[\text{Ca}^{2+}]_i$  is elevated during  $V_m$  depolarisation, leading to activation of KSper and consequent  
403 repolarisation. Such  $V_m$ -regulated, cyclic  $\text{Ca}^{2+}$  influx has been described in a diverse range of cell  
404 types, occurring either as periodic action potential bursts (Cornelisse, et al., 2001, Gorman and  
405 Thomas, 1978, Schlegel, et al., 1987) or repeated depolarising excursions of  $V_m$  (Ferrier, et al., 1987,  
406 Lopez, et al., 2014). However, some aspects of P4-induced oscillations reported here and elsewhere  
407 appear inconsistent with this simple model and require further investigation. Firstly, in the presence of  
408 valinomycin any effects of KSper currents on  $V_m$  will be damped, both because of the increased  
409 constitutive  $\text{K}^+$  'leak' and because valinomycin sets  $V_m$  at or close to  $E_K$  (figure S3). Though most

410 oscillations are inhibited, some cells, particularly with  $[K^+]_o = 100$  mM, continue to generate small  
411  $[Ca^{2+}]_i$  oscillations. Secondly, we observed previously that following stimulation with P4,  $\approx 50\%$  of  
412 oscillating cells continue to oscillate (or restart) after P4 washout (Harper et al, 2004), even though  
413 P4-withdrawal will cause a +ve shift in voltage sensitivity of CatSper (Lishko, et al., 2011).

414 Other potential causes of/contributors to generation of  $[Ca^{2+}]_i$  oscillations include regulation of  
415 CatSper activity by oscillation of  $pH_i$ . Feedback mechanisms involving fluctuations of  $V_m$  and  $pH_i$   
416 have been proposed to underlie the trains of  $[Ca^{2+}]_i$  spikes that occur in the flagellum of sea urchin  
417 sperm (Priego-Espinosa, et al., 2020, Wood, et al., 2003). These  $[Ca^{2+}]_i$  signals, similarly to those  
418 investigated here, initiate in the flagellum and are inhibited by manipulation of  $V_m$ , though their  
419 kinetics are strikingly different (Wood, et al., 2003). In human sperm the voltage dependent  $H^+$   
420 channel Hv1 is expressed (Lishko, et al., 2010) and thus depolarisation of  $V_m$  might lead indirectly to  
421 CatSper activation via  $H^+$  efflux and cytoplasmic alkalinisation (Lishko and Kirichok, 2010).  
422 However, human KSper shows low sensitivity to  $pH_i$  (Brenker, et al., 2014) and capacitation and  
423 incubation at acid pH ( $pH_o=6.5$ ), conditions which would significantly reduce the value of  $pH_i$  that  
424 might be achieved upon activation of Hv1, increased both the occurrence (% cells) and size of  $[Ca^{2+}]_i$   
425 oscillations in human sperm (Mata-Martinez, et al., 2018).

426  $[Ca^{2+}]_i$  oscillations and fertility. With regard to the potential clinical significance of these  
427 observations, a recent study on cells used for IVF showed that the occurrence of oscillating cells was  
428 low in samples that failed to fertilise. In particular, the proportion of samples where no oscillating  
429 cells were observed was significantly greater in non-fertilising samples than in samples from patients  
430 where fertilisation was successful (Kelly, et al., 2018). This suggests that failure of oscillations  
431 themselves, or of the physiological processes that generate them, may underlie some instances of  
432 idiopathic infertility. Oscillations appear to be involved in regulation of flagellar activity and  
433 acrosome reaction (see introduction) so their failure could well result in a reduced chance of  
434 fertilisation, both *in vivo* and in IVF. With regard to the underlying physiological mechanisms,  
435 complete loss of CatSper expression or function appears to be rare, even in sperm of subfertile men  
436 (Brown, et al., 2019), but either reduced functional expression of CatSper (Tamburrino, et al., 2015;

437 Marchiani, et al., 2017) or impaired regulation of  $V_m$  (Brown et al., 2016) might result in failure to  
438 generate  $[Ca^{2+}]_i$  oscillations. Detection of the occurrence of oscillations as a component of routine  
439 semen assessment clearly is impractical, since they can be observed only by time-lapse fluorescence  
440 imaging, but further studies on their generation, regulation and functional significance may well throw  
441 light on key aspects of the fertilisation process.

442

#### 443 **Authors' roles**

444 E.T., S.G. and E.M-M. carried out the laboratory work. E.T., S.G. E.M-M. and S.P. analysed  
445 the data. All authors contributed to writing and/or editing of the ms.

#### 446 **Funding**

447 ET-N was in receipt of a postgraduate scholarship from the CAPES Foundation (Ministry of  
448 Education, Brazil).

#### 449 **Conflict of interest**

450 The authors have no conflicts of interest.

451

452

453 **References**

- 454 Achikanu C, Pendekanti V, Teague R, Publicover S. Effects of pH manipulation, CatSper stimulation  
455 and  $\text{Ca}^{2+}$ -store mobilization on  $[\text{Ca}^{2+}]_i$  and behaviour of human sperm. *Hum Reprod* 2018;33: 1802-  
456 1811.
- 457 Alasmari W, Costello S, Correia J, Oxenham SK, Morris J, Fernandes L, Ramalho-Santos J, Kirkman-  
458 Brown J, Michelangeli F, Publicover S *et al.*  $\text{Ca}^{2+}$  signals generated by CatSper and  $\text{Ca}^{2+}$  regulate  
459 different behaviours in human sperm. *J Biol Chem* 2013;288: 6248-6258.
- 460 Bedu-Addo K, Barratt CL, Kirkman-Brown JC, Publicover SJ. Patterns of  $[\text{Ca}^{2+}]_i$  mobilization and  
461 cell response in human spermatozoa exposed to progesterone. *Dev Biol* 2007;302: 324-332.
- 462 Berridge MJ, Bootman MD, Roderick HL. Calcium signalling: dynamics, homeostasis and  
463 remodelling. *Nat Rev Mol Cell Biol* 2003;4: 517-529.
- 464 Berridge MJ, Cobbold PH, Cuthbertson KS. Spatial and temporal aspects of cell signalling. *Philos*  
465 *Trans R Soc Lond B Biol Sci* 1988;320: 325-343.
- 466 Brenker C, Zhou Y, Muller A, Echeverry F, Trotschel C, Poetsch A, Xia X, Bonigk W, Lingle C,  
467 Kaupp U *et al.* Slo3 in human sperm - a  $\text{K}^+$  channel activated by  $\text{Ca}^{2+}$  *ELife* 2014;3:e01438.
- 468 Brown SG, Costello S, Kelly MC, Ramalingam M, Drew E, Publicover SJ, Barratt CLR, Martins Da  
469 Silva S. Complex CatSper-dependent and independent  $[\text{Ca}^{2+}]_i$  signalling in human spermatozoa  
470 induced by follicular fluid. *Hum Reprod* 2017;32: 1995-2006.
- 471 Brown SG, Publicover SJ, Barratt CL, Martins da Silva S. Human sperm ion channel  
472 (dys)function: implications for fertilization. *Human Reproduction Update* 2019; 25, 758–776.
- 473 Brown SG, Publicover SJ, Mansell SA, Lishko PV, Williams HL, Ramalingam M, Wilson SM,  
474 Barratt CL, Sutton KA, Martins Da Silva S. Depolarization of sperm membrane potential is a  
475 common feature of men with subfertility and is associated with low fertilization rate at IVF. *Hum*  
476 *Reprod* 2016;31: 1147-1157.
- 477 Cai X, Clapham DE. Evolutionary genomics reveals lineage-specific gene loss and rapid evolution of  
478 a sperm-specific ion channel complex: CatSper and CatSperbeta. *PLoS One* 2008;3: e3569.

- 479 Cornelisse LN, Scheenen WJ, Koopman WJ, Roubos EW, Gielen SC. Minimal model for intracellular  
480 calcium oscillations and electrical bursting in melanotrope cells of *Xenopus laevis*. *Neural Comput*  
481 2001;13: 113-137.
- 482 Correia J, Michelangeli F, Publicover S. Regulation and roles of  $\text{Ca}^{2+}$  stores in human sperm.  
483 *Reproduction (Cambridge, England)* 2015;150: R65-76.
- 484 Costello S, Michelangeli F, Nash K, Lefievre L, Morris J, Machado-Oliveira G, Barratt C, Kirkman-  
485 Brown J, Publicover S.  $\text{Ca}^{2+}$  stores in sperm: their identities and functions. *Reproduction* 2009;138:  
486 425-437.
- 487 Darszon A, Nishigaki T, Beltran C, Trevino CL. Calcium channels in the development, maturation,  
488 and function of spermatozoa. *Physiol Rev* 2011;91: 1305-1355.
- 489 Felber SM, Brand MD. Valinomycin can depolarize mitochondria in intact lymphocytes without  
490 increasing plasma membrane potassium fluxes. *FEBS Lett* 1982;150: 122-124.
- 491 Ferrier J, Ward-Kesthely A, Homble F, Ross S. Further analysis of spontaneous membrane potential  
492 activity and the hyperpolarizing response to parathyroid hormone in osteoblastlike cells. *J Cell*  
493 *Physiol* 1987;130: 344-351.
- 494 Fraire-Zamora JJ, Gonzalez-Martinez MT. Effect of intracellular pH on depolarization-evoked  
495 calcium influx in human sperm. *Am J Physiol Cell Physiol* 2004;287: C1688-1696.
- 496 Gorman AL, Thomas MV. Changes in the intracellular concentration of free calcium ions in a pace-  
497 maker neurone, measured with the metallochromic indicator dye arsenazo III. *J Physiol* 1978;275:  
498 357-376.
- 499 Guerrero A, Nishigaki T, Carneiro J, Yoshiro T, Wood CD, Darszon A. Tuning sperm chemotaxis by  
500 calcium burst timing. *Dev Biol* 2010;344: 52-65.
- 501 Harper CV, Barratt CL, Publicover SJ. Stimulation of human spermatozoa with progesterone  
502 gradients to simulate approach to the oocyte. Induction of  $[\text{Ca}^{2+}]_i$  oscillations and cyclical  
503 transitions in flagellar beating. *J Biol Chem* 2004;279: 46315-46325.
- 504 Kaupp UB, Kashikar ND, Weyand I. Mechanisms of sperm chemotaxis. *Annu Rev Physiol* 2008;70:  
505 93-117.



- 506 Kelly MC, Brown SG, Costello SM, Ramalingam M, Drew E, Publicover SJ, Barratt CLR, Martins  
507 Da Silva S. Single-cell analysis of  $[Ca^{2+}]_i$  signalling in sub-fertile men: characteristics and relation to  
508 fertilization outcome. *Hum Reprod* 2018;33: 1023-1033.
- 509 Linares-Hernandez L, Guzman-Grenfell AM, Hicks-Gomez JJ, Gonzalez-Martinez MT. Voltage-  
510 dependent calcium influx in human sperm assessed by simultaneous optical detection of intracellular  
511 calcium and membrane potential. *Biochim Biophys Acta* 1998;1372: 1-12.
- 512 Lishko PV, Botchkina IL, Fedorenko A, Kirichok Y. Acid extrusion from human spermatozoa  
513 is mediated by flagellar voltage-gated proton channel. *Cell* 2010;140: 327–337,
- 514 Lishko PV, Botchkina IL, Kirichok Y. Progesterone activates the principal  $Ca^{2+}$  channel of human  
515 sperm. *Nature* 2011;471: 387-391.
- 516 Lishko PV, Kirichok Y. The role of Hv1 and CatSper channels in sperm activation. *J Physiol*  
517 2010;588: 4667-4672.
- 518 Lopez MG, Artalejo AR, Garcia AG, Neher E, Garcia-Sancho J. Veratridine-induced oscillations of  
519 cytosolic calcium and membrane potential in bovine chromaffin cells. *J Physiol* 1995;482 ( Pt 1): 15-  
520 27.
- 521 Machado-Oliveira G, Lefievre L, Ford C, Herrero MB, Barratt C, Connolly TJ, Nash K, Morales-  
522 Garcia A, Kirkman-Brown J, Publicover S. Mobilisation of  $Ca^{2+}$  stores and flagellar regulation in  
523 human sperm by S-nitrosylation: a role for NO synthesised in the female reproductive tract.  
524 *Development* 2008;135: 3677-3686.
- 525 Mannowetz N, Naidoo N, Choo S-AS, Smith JF, Lishko PV. Slo1 is the principal potassium channel of  
526 human spermatozoa. *eLife* 2013; PMID: 24137539 DOI: 10.7554/eLife.01009
- 527 Mansell SA, Publicover SJ, Barratt CL, Wilson SM. Patch clamp studies of human sperm under  
528 physiological ionic conditions reveal three functionally and pharmacologically distinct cation  
529 channels. *Mol Hum Reprod* 2014; 20: 392-408.
- 530 Marchiani S, Tamburrino L, Benini F, Fanfani L, Dolce R, Rastrelli G, Maggi M, Pellegrini S, Baldi  
531 E. Chromatin Protamination and Catsper Expression in Spermatozoa Predict Clinical Outcomes after  
532 Assisted Reproduction Programs. *Sci Rep* 2017 7:15122.

- 533 Mata-Martinez E, Darszon A, Trevino CL. pH-dependent Ca<sup>2+</sup> oscillations prevent untimely  
534 acrosome reaction in human sperm. *Biochem Biophys Res Commun* 2018;497: 146-152.
- 535 Mizutani H, Yamamura H, Muramatsu M, Kiyota K, Nishimura K, Suzuki Y, Ohya S, Imaizumi Y.  
536 Spontaneous and nicotine-induced Ca<sup>2+</sup> oscillations mediated by Ca<sup>2+</sup> influx in rat pinealocytes. *Am J*  
537 *Physiol Cell Physiol* 2014;306: C1008-1016.
- 538 Nash K, Lefievre L, Peralta-Arias R, Morris J, Morales-Garcia A, Connolly T, Costello S, Kirkman-  
539 Brown JC, Publicover SJ. Techniques for imaging Ca<sup>2+</sup> signaling in human sperm. *J Vis Exp* 2010:  
540 doi:pri: 1996. 1910.3791/1996.
- 541 Olson SD, Suarez SS, Fauci LJ. A model of CatSper channel mediated calcium dynamics in  
542 mammalian spermatozoa. *Bull Math Biol* 2010;72: 1925-1946.
- 543 Priego-Espinosa DA, Darszon A, Guerrero A, Gonzalez-Cota AL, Nishigaki T, Martinez-Mekler G,  
544 Carneiro J. Modular analysis of the control of flagellar Ca<sup>2+</sup>-spike trains produced by CatSper and  
545 CaV channels in sea urchin sperm. *PLoS Comput Biol* 2020;16: e1007605.
- 546 Publicover S. Regulation of Sperm Behaviour: The Role(s) of [Ca<sup>2+</sup>]<sub>i</sub> Signalling. In De Jonge CJD,  
547 Barratt. CLR (ed) *The Sperm Cell, Second Edition*. 2017. Cambridge University Press, Cambridge  
548 UK, pp. 126-142.
- 549 Publicover S, Harper CV, Barratt C. [Ca<sup>2+</sup>]<sub>i</sub> signalling in sperm--making the most of what you've got.  
550 *Nat Cell Biol* 2007;9: 235-242.
- 551 Ren D, Navarro B, Perez G, Jackson AC, Hsu S, Shi Q, Tilly JL, Clapham DE. A sperm ion channel  
552 required for sperm motility and male fertility. *Nature* 2001;413: 603-609.
- 553 Rennhack A, Schiffer C, Brenker C, Fridman D, Nitao ET, Cheng YM, Tamburrino L, Balbach M,  
554 Stolting G, Berger TK *et al*. A novel cross-species inhibitor to study the function of CatSper Ca<sup>(2+)</sup>  
555 channels in sperm. *Br J Pharmacol* 2018;175: 3144-3161.
- 556 Salvioli S, Barbi C, Dobrucki J, Moretti L, Pinti M, Pedrazzi J, Paziienza TL, Bobyleva V, Franceschi  
557 C, Cossarizza A. Opposite role of changes in mitochondrial membrane potential in different apoptotic  
558 processes. *FEBS Lett* 2000;469: 186-190.

- 559 Sanchez-Cardenas C, Servin-Vences MR, Jose O, Trevino CL, Hernandez-Cruz A, Darszon A.  
560 Acrosome reaction and  $\text{Ca}^{2+}$  imaging in single human spermatozoa: new regulatory roles of  $[\text{Ca}^{2+}]_i$ .  
561 *Biol Reprod* 2014;91: 67.
- 562 Santi SM, Martínez-López P, de la Vega-Beltrán JL, Butler A, Alisio A, Darszon A, Salkoff L. The  
563 SLO3 sperm-specific potassium channel plays a vital role in male fertility. *FEBS Lett* 2010;  
564 584:1041–1046
- 565 Schiffer C, Muller A, Egeberg DL, Alvarez L, Brenker C, Rehfeld A, Frederiksen H, Waschle B,  
566 Kaupp UB, Balbach M *et al.* Direct action of endocrine disrupting chemicals on human sperm. *EMBO*  
567 *Rep* 2014;15: 758-765.
- 568 Schlegel W, Winiger BP, Mollard P, Vacher P, Wuarin F, Zahnd GR, Wollheim CB, Dufy B.  
569 Oscillations of cytosolic  $\text{Ca}^{2+}$  in pituitary cells due to action potentials. *Nature* 1987;329: 719-721.
- 570 Seifert R, Flick M, Bonigk W, Alvarez L, Trotschel C, Poetsch A, Muller A, Goodwin N, Pelzer P,  
571 Kashikar ND *et al.* The CatSper channel controls chemosensation in sea urchin sperm. *The EMBO*  
572 *journal* 2015;34: 379-392.
- 573 Servin-Vences MR, Tatsu Y, Ando H, Guerrero A, Yumoto N, Darszon A, Nishigaki T. A caged  
574 progesterone analog alters intracellular  $\text{Ca}^{2+}$  and flagellar bending in human sperm. *Reproduction*  
575 2012;144: 101-109.
- 576 Smith JF, Syrityna O, Fellous M, Serres C, Mannowetz N, Kirichok Y, Lishko PV. Disruption of the  
577 principal, progesterone-activated sperm  $\text{Ca}^{2+}$  channel in a CatSper2-deficient infertile patient. *Proc*  
578 *Natl Acad Sci U S A* 2013;110: 6323-6328.
- 579 Suarez SS. Control of hyperactivation in sperm. *Hum Reprod Update* 2008;14: 647-657.
- 580 Tamburrino L, Marchiani S, Vicini E, Muciaccia B, Cambi M, Pellegrini S, Forti G, Muratori M,  
581 Baldi E. Quantification of CatSper1 expression in human spermatozoa and relation to functional  
582 parameters. *Hum Reprod* 2015; 30:1532-1544. doi: 10.1093
- 583 Wood CD, Darszon A, Whitaker M. Spermact induces calcium oscillations in the sperm tail. *J Cell Biol*  
584 2003;161: 89-101.
- 585 World Health Organization DoRHAR. WHO laboratory manual for the examination and processing of  
586 human semen Fifth edition, 2010. World Health Organization.

587 Zeng X-H, Yang C, Kim ST, Lingle CJ, and Xia XM P Deletion of the Slo3 gene abolishes  
588 alkalization-activated K<sup>+</sup> current in mouse spermatozoa. *Proc Natl Acad Sci U S A* 2011;108: 5879–  
589 5884  
590  
591

592 **Figure legends**

593 **Figure 1. Site of initiation and  $[Ca^{2+}]_o$ -sensitivity of  $[Ca^{2+}]_i$  oscillations. a)**  $[Ca^{2+}]_i$  oscillation  
 594 recorded in the principal piece (black trace) neck (red) and head (grey) of a single sperm. The  $[Ca^{2+}]_i$   
 595 increase occurs first in the principal piece but signals in the neck and head are larger. Traces show %  
 596 increase in fluo4 fluorescence intensity with respect to mean fluorescence before the progesterone  
 597 (P4) stimulus ( $\Delta$  fluorescence (%)). **b)** Mean latency of  $[Ca^{2+}]_i$  responses in the neck (red) and head  
 598 (grey) compared to those in the flagellum. Left panel shows mean $\pm$ SEM (n=17 cells) for  $[Ca^{2+}]_i$   
 599 oscillations, right panel shows mean $\pm$ SEM (n=17 cells) for the preceding P4-induced  $[Ca^{2+}]_i$   
 600 transients. Latencies of both oscillations and transients to the neck and head were similar ( $P>0.2$ ) but  
 601 all significantly exceeded zero (Wilcoxon) \*\*\* $p<0.001$ . **c)** Mean amplitude  $\pm$ SEM (n=17 cells) of  
 602  $[Ca^{2+}]_i$  oscillations recorded in the distal flagellum (black), sperm neck (red) and head (grey)  
 603 normalised to amplitude in the proximal flagellum (black). Letters indicate statistically similar  
 604 amplitudes. Amplitudes in the head and neck significantly exceeded those in the flagellum  $P=2.2*10^{-5}$ ;  
 605 ANOVA with Tukey post hoc comparison. **d)** Mean amplitude  $\pm$ SEM (n=17 cells) of P4-induced  
 606  $[Ca^{2+}]_i$  transients recorded in the distal flagellum (black), sperm neck (red) and head (grey)  
 607 normalised to amplitude in the proximal flagellum (black). Amplitudes did not differ significantly  
 608 ( $P=0.67$ ; ANOVA). **e)** Responses of 5 individual cells to stimulation with 3  $\mu$ M P4 (arrow), followed  
 609 by superfusion with P4-containing 'Ca<sup>2+</sup>-free' saline ( $[Ca^{2+}]<5 \mu$ M; blue shading) for 30 min. EGTA-  
 610 buffered saline (calculated  $[Ca^{2+}]=2.6*10^{-10}$ M; grey shading) was then superfused for 10 min before  
 611 returning to 'Ca<sup>2+</sup>-free' saline and then to standard sEBSS. Note that oscillations arrest in 'Ca<sup>2+</sup>-free'  
 612 saline, before application of EGTA buffer.

613 **Figure 2. Valinomycin shifts membrane potential (Vm) to  $E_K$ .** **a)** Current clamp recording of Vm  
 614 in a single sperm. Grey shading shows periods of superfusion with 1  $\mu$ M valinomycin in standard (5.4  
 615 mM K<sup>+</sup>) saline. Red shading shows period of superfusion with 1  $\mu$ M valinomycin in depolarising (100  
 616 mM K<sup>+</sup>) saline. **b)** Recorded membrane potential (mean $\pm$ SEM) for cells under control conditions

617 (black; n=6 cells), exposed to 1  $\mu\text{M}$  valinomycin in standard (5.4 mM  $\text{K}^+$ ) saline (grey; n=5 cells) and  
618 exposed to 1  $\mu\text{M}$  valinomycin in depolarising (100 mM  $\text{K}^+$ ) saline (red; n=5 cells).

619 **Figure 3. Valinomycin does not inhibit the P4-induced  $[\text{Ca}^{2+}]_i$  transient.** **a)** Mean response to  
620 application of 3  $\mu\text{M}$  P4 (arrow) in the presence of valinomycin (red trace) and in parallel control  
621 experiments (black trace), n=7 experiments for each condition. Baseline of the valinomycin trace has  
622 been adjusted to facilitate comparison with the control trace. **b)** Mean amplitude ( $\pm\text{SEM}$ ) of the  
623  $[\text{Ca}^{2+}]_i$  transient recorded in the presence of valinomycin (red) and in its absence (black; n=8  
624 experiments for each condition)  $P=0.95$ , paired t). **c)** Application 1  $\mu\text{M}$  valinomycin (grey shading)  
625 causes a small, sustained increase in  $[\text{Ca}^{2+}]_i$ . Subsequent application of 3  $\mu\text{M}$  P4 (arrow) induced a  
626  $[\text{Ca}^{2+}]_i$  transient but oscillations occurred only after washout of valinomycin. Oscillations arrested or  
627 paused upon washout of P4 (upward arrow). Responses of 4 separate cells shown.  $[\text{K}^+]_o = 5.4$  mM  
628 throughout.

629 **Figure 4. Effect of valinomycin on  $[\text{Ca}^{2+}]_i$  oscillations.** Cells were stimulated with 3  $\mu\text{M}$  P4 (arrow)  
630 to induce oscillations then exposed to 1  $\mu\text{M}$  valinomycin (shown by grey shading). **a)**  $[\text{K}^+]_o = 5.4$   
631 mM, (estimated  $E_K = -78.1$  mV). **b)** during valinomycin exposure  $[\text{K}^+]_o$  was increased to 25 mM  
632 (estimated  $E_K = -39.5$  mV). **c)** during valinomycin exposure  $[\text{K}^+]_o$  was increased to 100 mM (estimated  
633  $E_K = -4.6$  mV). Each panel shows responses of 5 individual cells.

634 **Figure 5. Effect of valinomycin on  $[\text{Ca}^{2+}]_i$  oscillations depends on  $[\text{K}^+]_o$ .** **a)** Proportion of  
635 oscillating cells in which activity was suppressed (shown by black shading) in the presence of 1  $\mu\text{M}$   
636 valinomycin varied with  $[\text{K}^+]_o$  (5.4 mM, n=257 cells; 25 mM, n=117 cells and 100 mM, n=114 cells;  
637  $P=10^{-25}$ ; chi-square). **b)** Amplitude of oscillations that persisted in the presence of valinomycin varied  
638 with  $[\text{K}^+]_o$ . Bars show mean ( $\pm\text{SEM}$ ) oscillation amplitude normalised to that during the control  
639 period (prior to valinomycin treatment, grey). 5.4 mM, n=9 cells; 25 mM, n=22 cells and 100 mM,  
640 n=22 cells. Asterisks indicate significant difference from control period, \*\*\*  $p<0.001$ , \*\*\*\*  $p<0.0001$   
641 (Paired t or Mann-Whitney). **c)** Frequency of oscillations that persisted in the presence of valinomycin  
642 varied with  $[\text{K}^+]_o$ . Bars show mean ( $\pm\text{SEM}$ ) oscillation frequency normalised to that during the

643 control period (prior to valinomycin treatment; grey). 5.4 mM, n=9 cells; 25 mM, n=22 cells and 100  
644 mM, n=22 cells. Asterisks indicate significant difference from control period, \*\*\*\* p<0.0001,  
645 (Paired-t or Mann-Whitney).

646 **Figure 6. RU1968 and quinidine inhibit  $[Ca^{2+}]_i$  oscillations.** Cells were stimulated with 3  $\mu$ M  
647 progesterone (P4; arrow) to induce oscillations then exposed to RU1968 or quinidine (shown by grey  
648 shading). **a)** Effect of 11  $\mu$ M RU1968. **b)** Effect of 4.8  $\mu$ M RU1968. **c)** Effect of 300  $\mu$ M quinidine.  
649 Each panel shows responses of 5 individual cells.

650 **Figure 7. Effect of RU1968 on incidence and characteristics of  $[Ca^{2+}]_i$  oscillations.** **a)** Proportion  
651 of cells in which oscillations were inhibited (shown by black shading) in the presence of 4.8  $\mu$ M  
652 (n=129 cells) and 11  $\mu$ M RU1968 (n=58 cells). **b)** Frequency of oscillations in cells in which activity  
653 persisted in the presence of 4.8  $\mu$ M RU1968 (red) was significantly decreased compared to preceding  
654 (control) period (grey; n=67 cells). **c)** Amplitude of oscillations in cells in which activity persisted in  
655 the presence of 4.8  $\mu$ M RU1968 (red) was significantly increased compared to preceding (control)  
656 period (grey n=67 cells). **d)** Duration of oscillations in cells in which activity persisted in the presence  
657 of 4.8  $\mu$ M RU1968 (red) was significantly increased compared to preceding (control) period (grey;  
658 n=73 cells). Asterisks indicate significant difference from control period, \*\*\*\*P<0.0001 (Paired-t or  
659 Mann-Whitney).

660

### 661 **Supplementary figure legends**

662 **Figure S1. Effective dose of RU1968 is reduced in superfusion experiments.** Dose-dependency of  
663 inhibition by RU1968 of the  $[Ca^{2+}]_i$  transient induced by 3  $\mu$ M progesterone in static chamber  
664 experiments (red,  $IC_{50}$ =6.9  $\mu$ M) and imaging experiments in the superfusion chamber (black,  
665  $IC_{50}$ =18.4  $\mu$ M). Points show mean  $\pm$ SEM of 3 or 4 experiments. Curve fitting and calculation of  $IC_{50}$   
666 were done using <https://mycurvefit.com/>. Arrows show estimation of effective concentrations applied  
667 in superfusion experiments.

668

669 **Figure S2.** Time-fluorescence plots for cells shown in videos 1-7. Arrows indicate time of application  
670 of 3  $\mu\text{M}$  progesterone (P4). **Panel a** shows rising phase of P4-induced  $[\text{Ca}^{2+}]_i$  transient (left ; video 1)  
671 and a subsequent  $[\text{Ca}^{2+}]_i$  oscillation (right ; video 2) in the same cell. Black traces show responses in  
672 proximal flagellum, red traces show responses in head. Amplitudes are scaled (minimum to  
673 maximum) to facilitate comparison of time-course. **Panels b, c and d** show % increase in fluo4  
674 fluorescence intensity with respect to mean fluorescence before the P4 stimulus ( $\Delta$  fluorescence (%))  
675 for the cells in videos 3, 4 and 5 respectively. Grey shading shows period of exposure to 1  $\mu\text{M}$   
676 valinomycin (panel b), 1  $\mu\text{M}$  valinomycin with 25 mM  $\text{K}^+$  (panel c) and 1  $\mu\text{M}$  valinomycin with 100  
677 mM  $\text{K}^+$  (panel d). **Panels e and f** show % increase in fluo4 fluorescence intensity with respect to  
678 mean fluorescence before the P4 stimulus ( $\Delta$  fluorescence (%)) for the cells in videos 6 and 7  
679 respectively. Grey shading shows period of exposure to 11  $\mu\text{M}$  RU1968 (panel e) and 4.8  $\mu\text{M}$  RU1968  
680 (panel f).

681

682 **Figure S3. Valinomycin sets  $V_m$  at  $E_K$ .** Calculated  $E_K$  and the directly measured  $V_m$  (zero current  
683 clamp) are plotted against  $\log [\text{K}^+]_o$ . Black line shows relationship of calculated  $E_K$  to  $[\text{K}^+]_o$ , red dotted  
684 line shows mean  $V_m$  ( $\pm$ SEM) in the presence of 5.4 mM and 100 mM  $[\text{K}^+]_o$ .

685

686 **Figure S4. RU1968 induces large, slow oscillation in some cells.** Application of 3  $\mu\text{M}$  P4 (arrow)  
687 induced a  $[\text{Ca}^{2+}]_i$  transient but no oscillations were seen in these cells. However, upon application of  
688 4.8  $\mu\text{M}$  RU1968 a large, slow  $[\text{Ca}^{2+}]_i$  oscillation was induced. Responses of 4 separate cells shown.  
689  $[\text{K}^+]_o = 5.4$  mM throughout.

690

691 **Video file legends**



692 **Video 1.**  $[Ca^{2+}]_i$  oscillation. 151 frames recorded at 2.5 Hz. 10 Hz playback.  $[Ca^{2+}]_i$  elevation in the  
693 flagellum precedes that in the head. Original image size (height\*width) = 37.6\*10.45  $\mu\text{m}$

694 **Video 2.** 3  $\mu\text{M}$  progesterone (P4)-induced  $[Ca^{2+}]_i$  transient, same cell as video 1. 151 frames recorded  
695 at 2.5 Hz. 10 Hz playback. P4 was applied at  $\approx 2$  s.  $[Ca^{2+}]_i$  elevation in the flagellum precedes that in  
696 the head. Original image size = 37.6\*10.45  $\mu\text{m}$

697 **Video 3.** Cell stimulated with P4 (5 min) then co-exposed to 1  $\mu\text{M}$  valinomycin (25-45 min). 840  
698 frames recorded at 0.2 Hz. 20 Hz playback. Original image size = 13.2\*22.4  $\mu\text{m}$

699 **Video 4.** Cell stimulated with P4 (5 min) then co-exposed to 1  $\mu\text{M}$  valinomycin and 25 mM  $K^+$  (25-45  
700 min). 840 frames recorded at 0.2 Hz. 20 Hz playback. Original image size = 24.4\*16.8  $\mu\text{m}$

701 **Video 5.** Cell stimulated with P4 (5 min) then co-exposed to 1  $\mu\text{M}$  valinomycin and 100 mM  $K^+$  (25-  
702 45 min). 840 frames recorded at 0.2 Hz. 20 Hz playback. Original image size = 15.2\*23.6  $\mu\text{m}$

703 **Video 6.** Cell stimulated with P4 (5 min) then co-exposed to 11  $\mu\text{M}$  RU1968 (16-26 min). 481 frames  
704 recorded at 0.2 Hz. 20 Hz playback. Original image size = 12.8\*24  $\mu\text{m}$

705 **Video 7.** Cell stimulated with P4 (3.3 min) then co-exposed to 4.8  $\mu\text{M}$  RU1968 (14-24 min). 433  
706 frames recorded at 0.2 Hz. 20 Hz playback. Original image size = 16.8\*16.8  $\mu\text{m}$

707

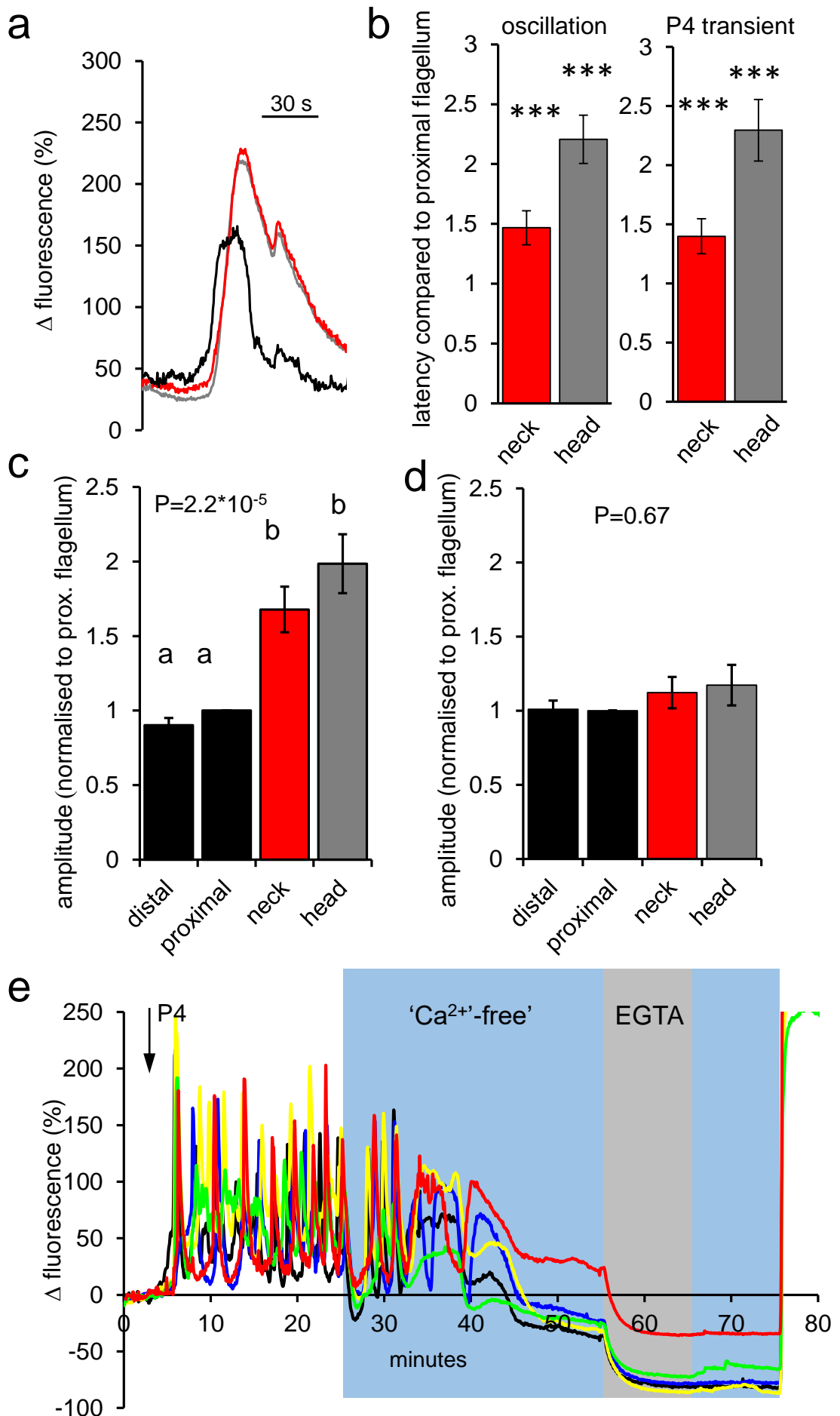


Fig 1

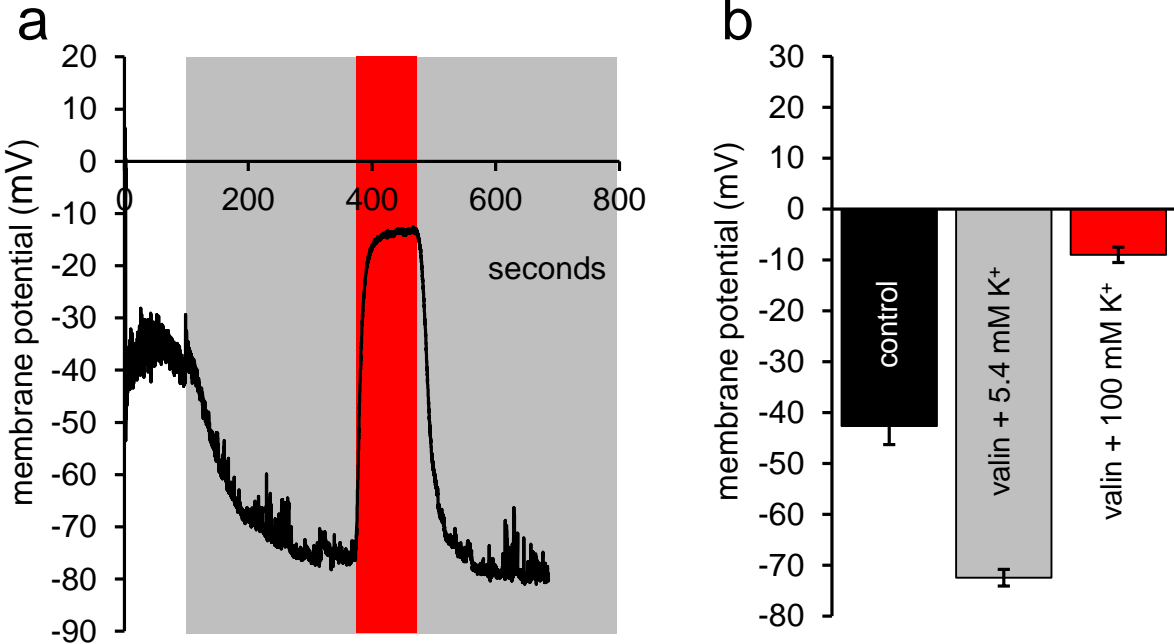


Fig 2

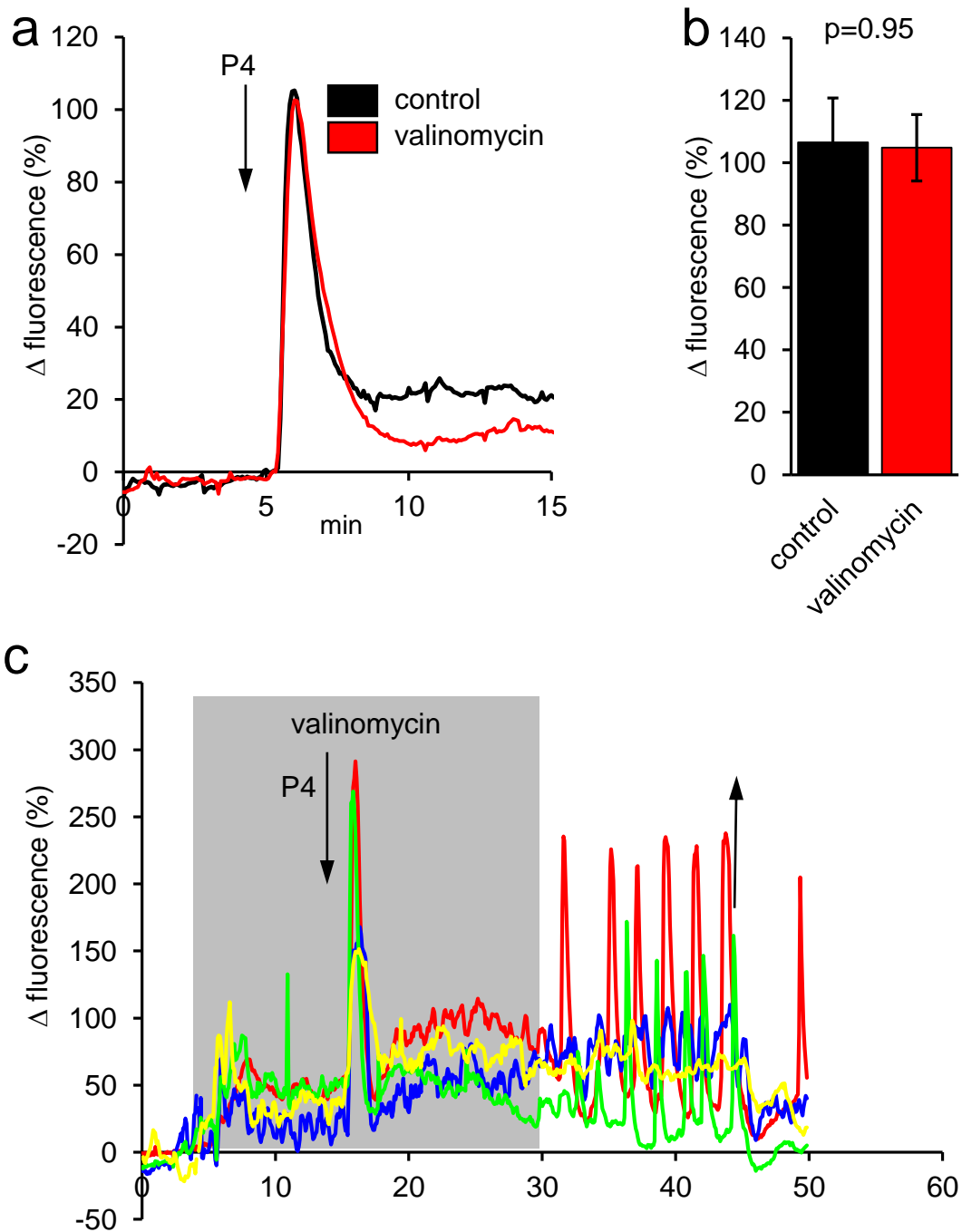


Fig 3

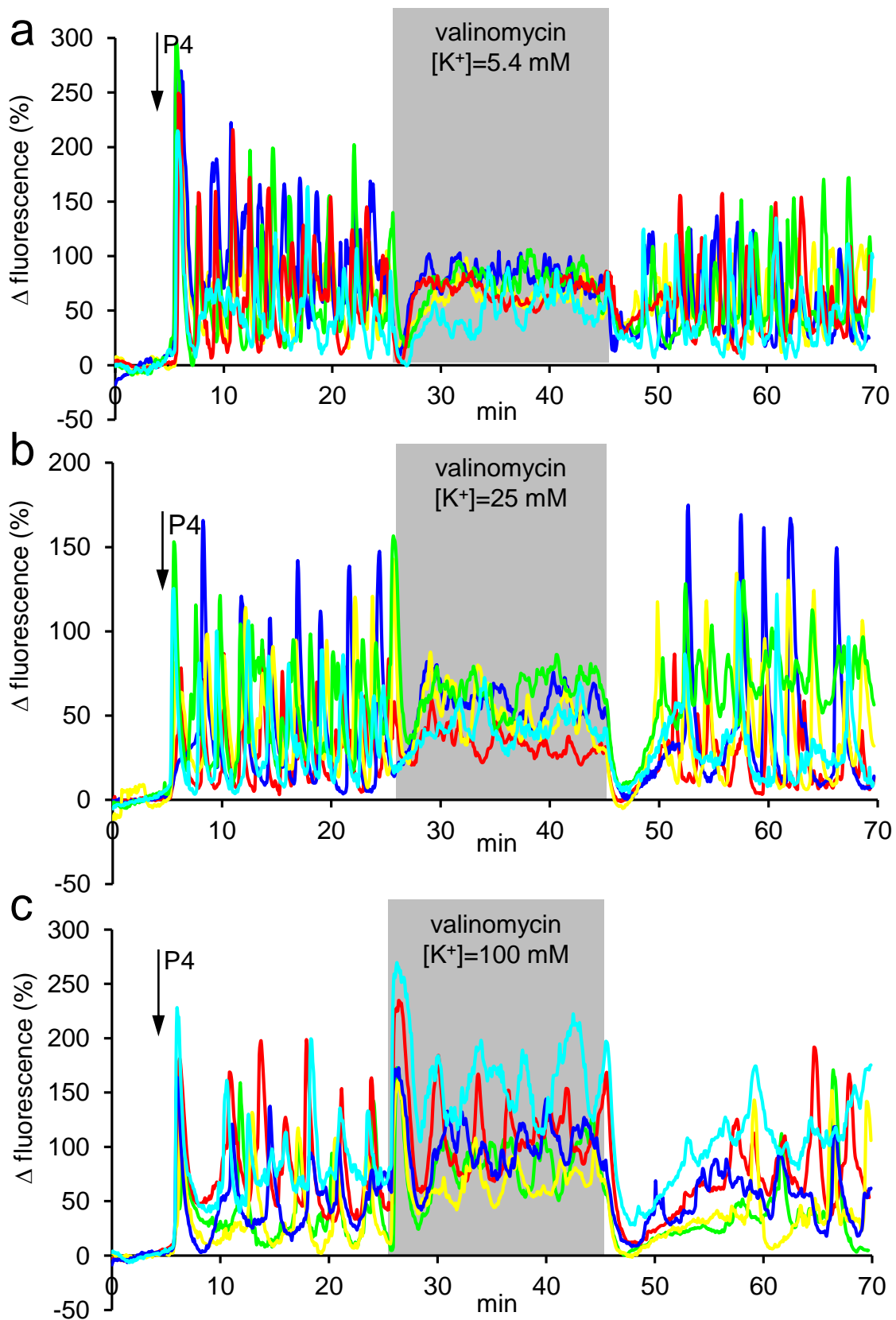


Fig 4

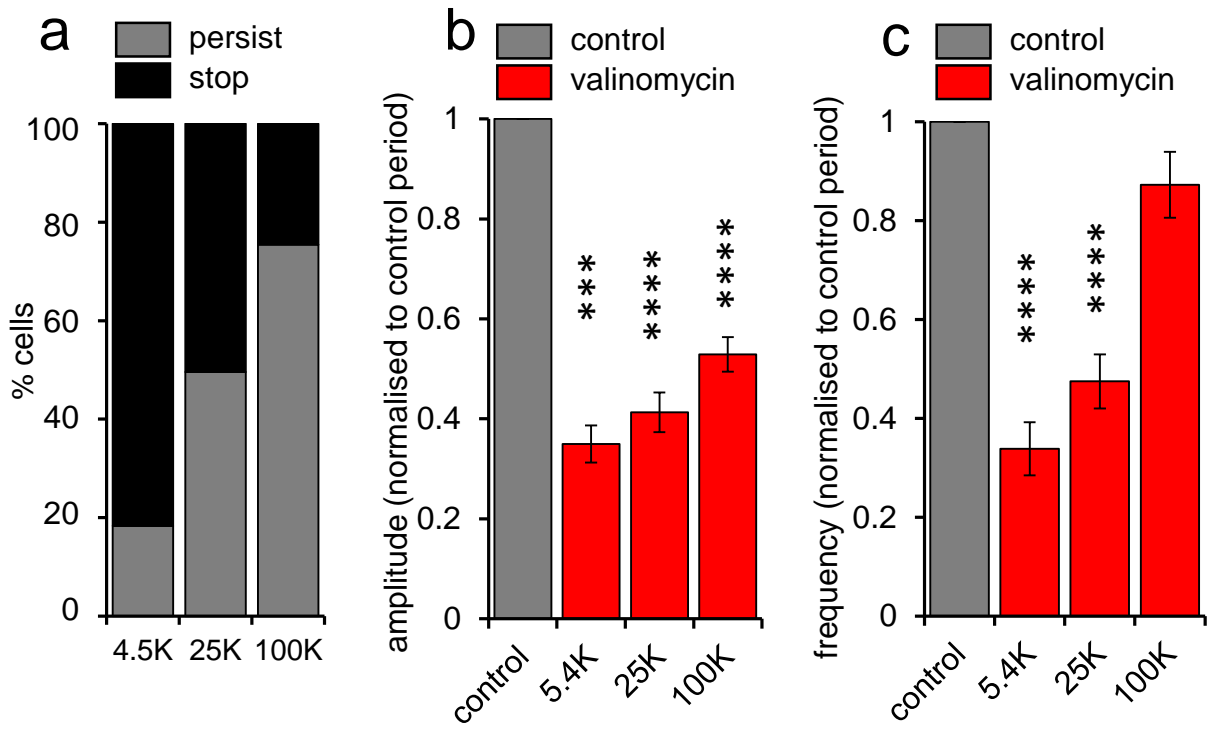


Fig 5

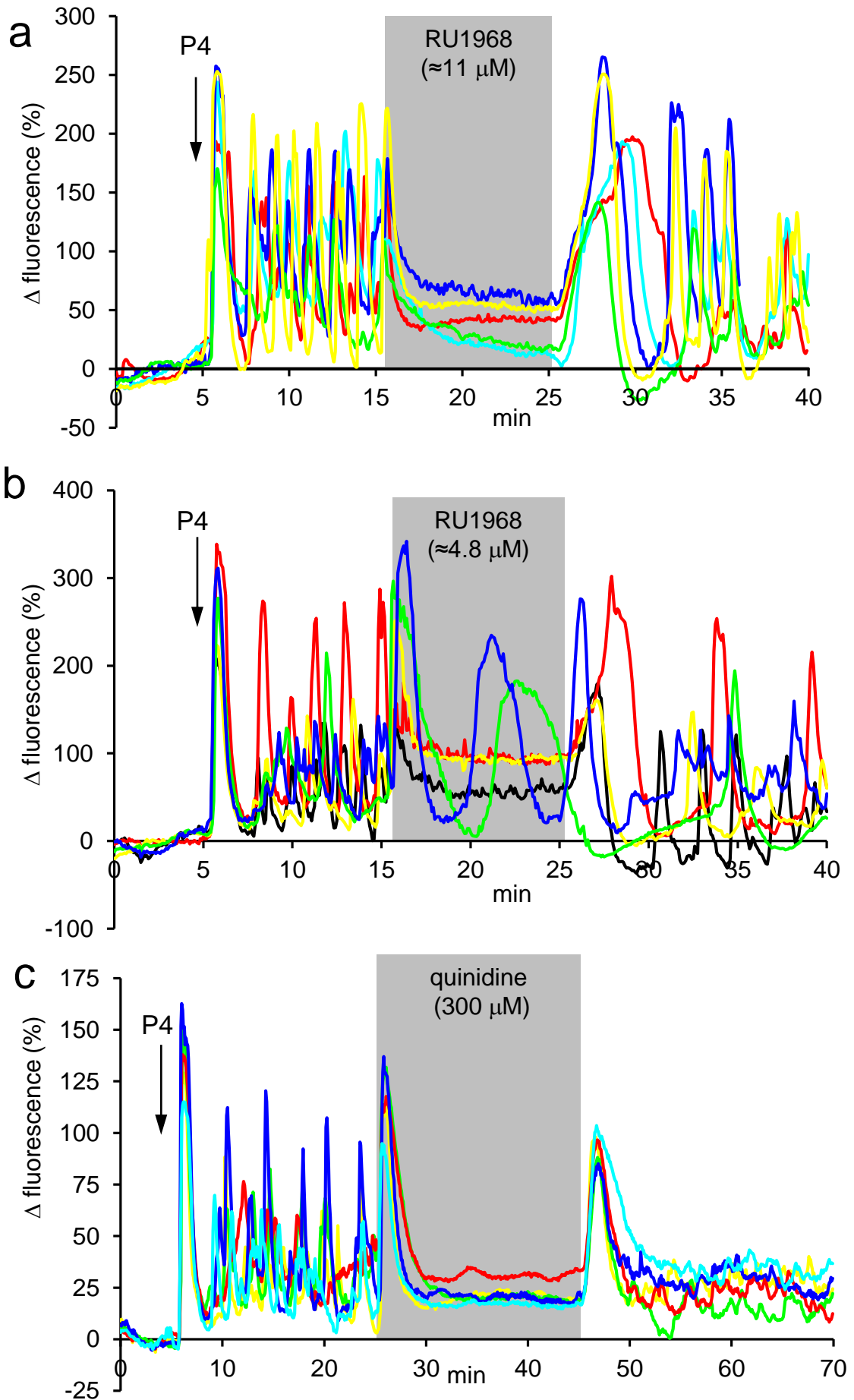


Fig 6

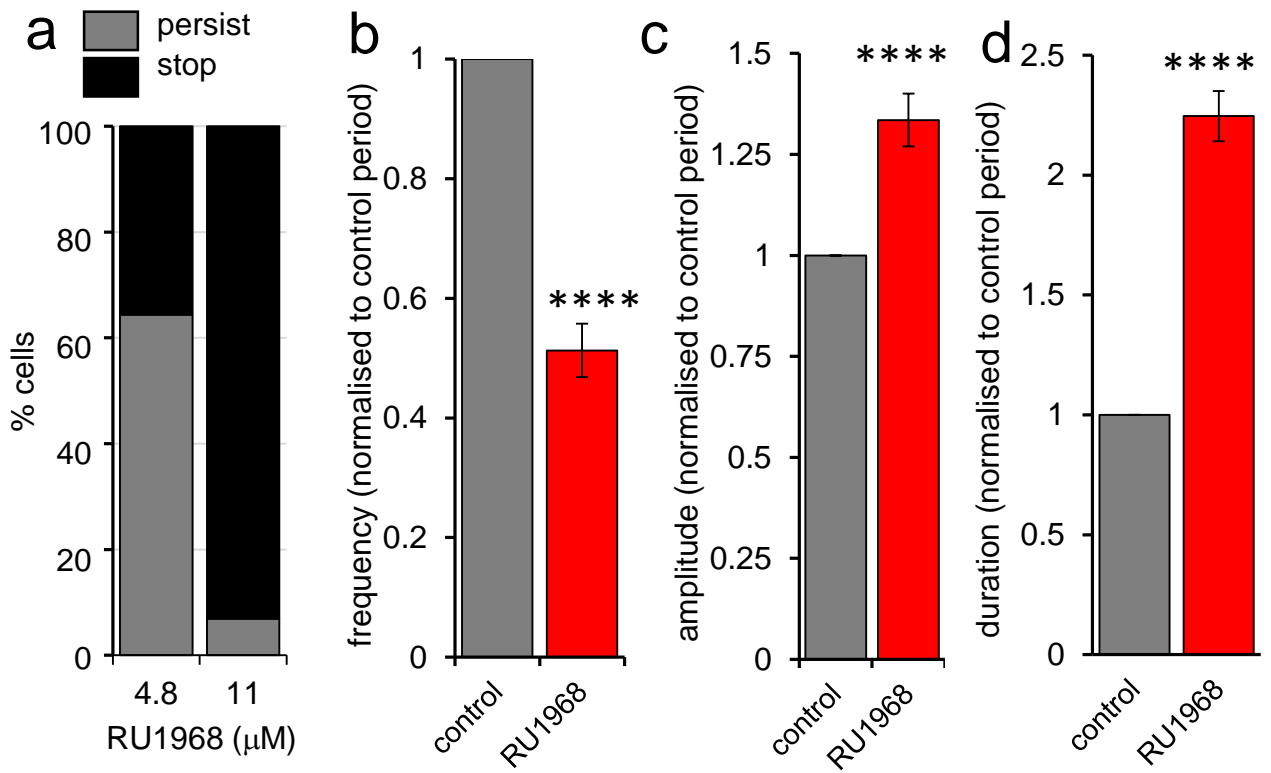


Fig 7



Table S1. Characteristics of semen samples and swim-up prepared samples

	semen			swim up		
	volume (ml)	concentration ( $10^6$ /ml)	total cells ( $\times 10^6$ )	total cells ( $\times 10^6$ )	total motile (%)	progressive motile (%)
median	3.00	94.30	255.20	45.00	90	68
5th centile	2.20	30.75	92.75	8.40	66	20
n	120	120	120	120	120	120

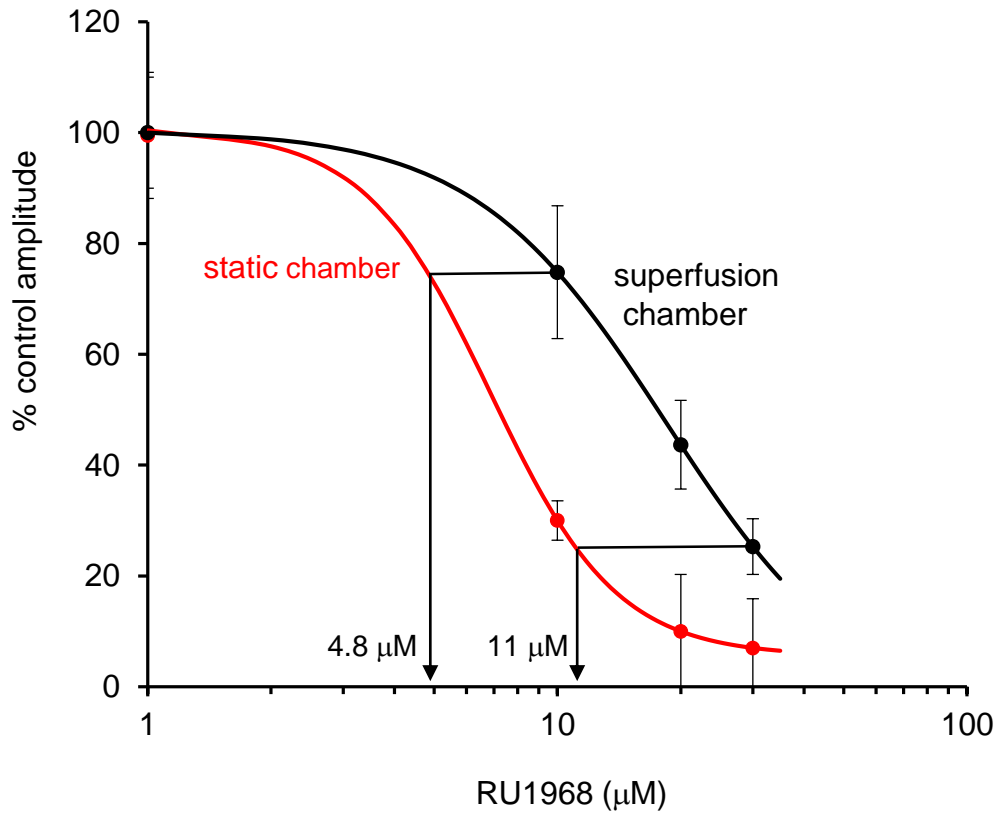


Fig S1

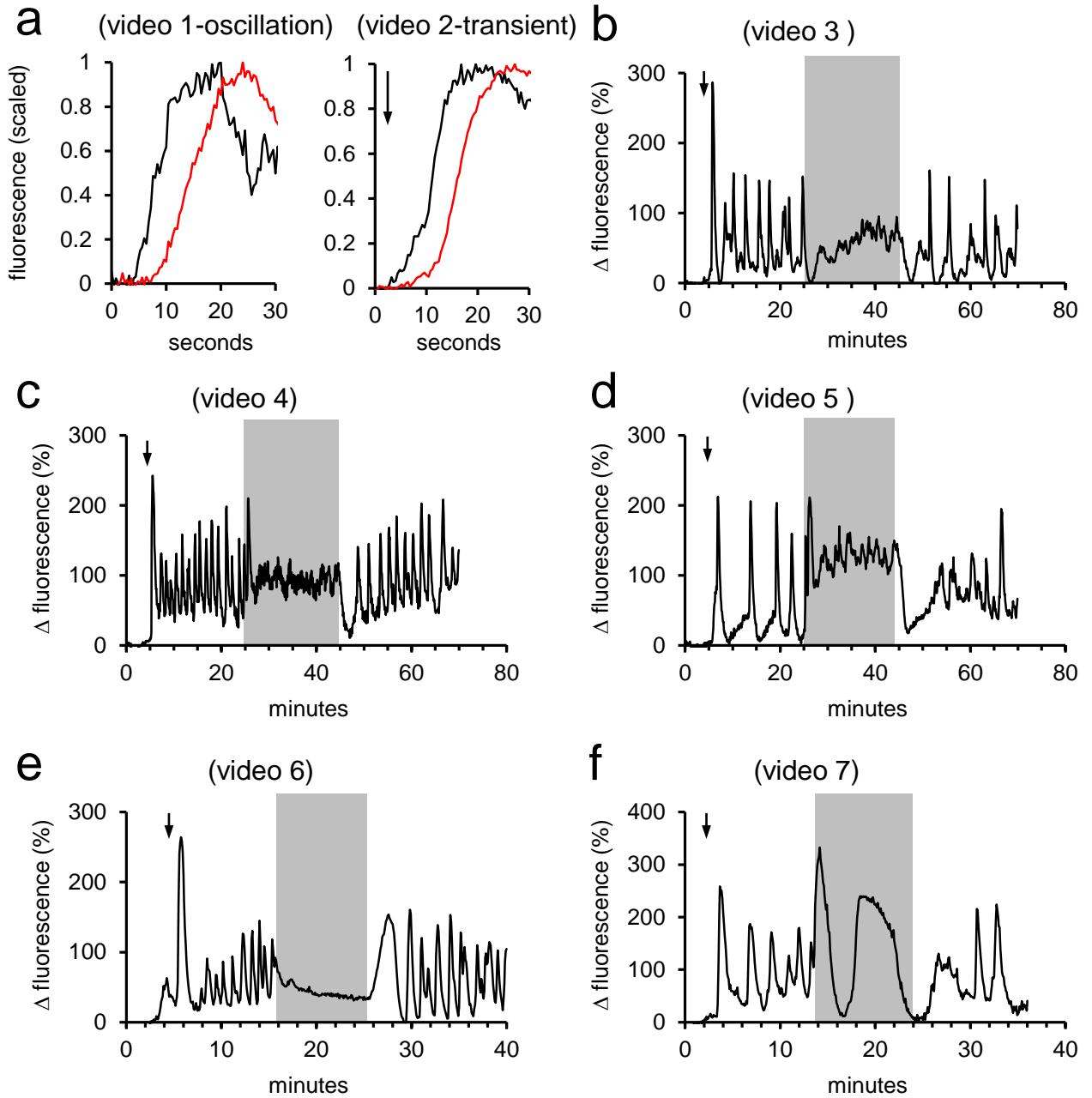


Fig S2

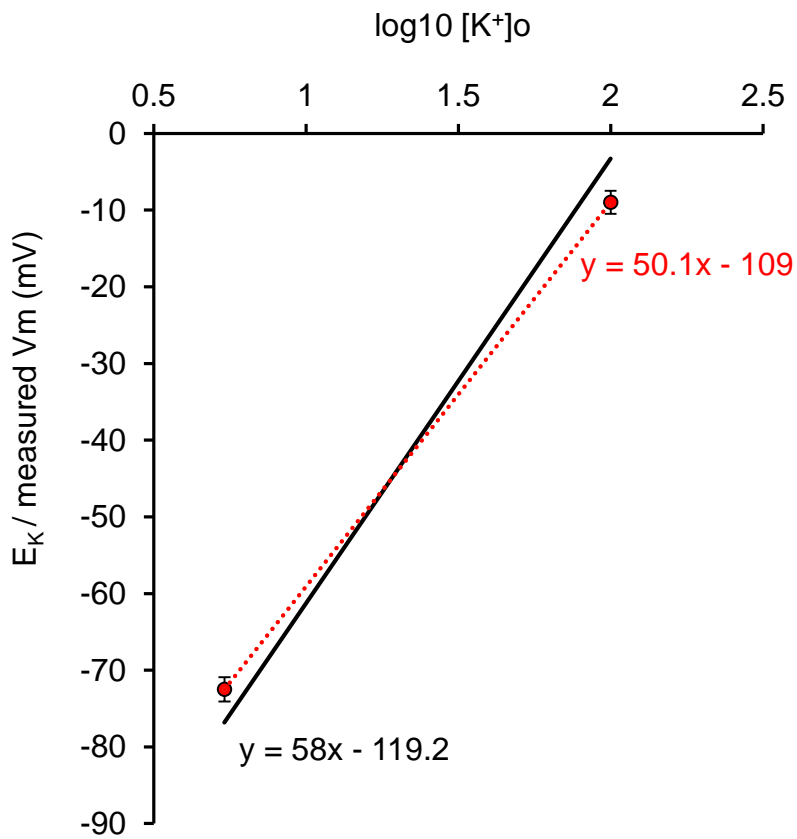


Fig S3

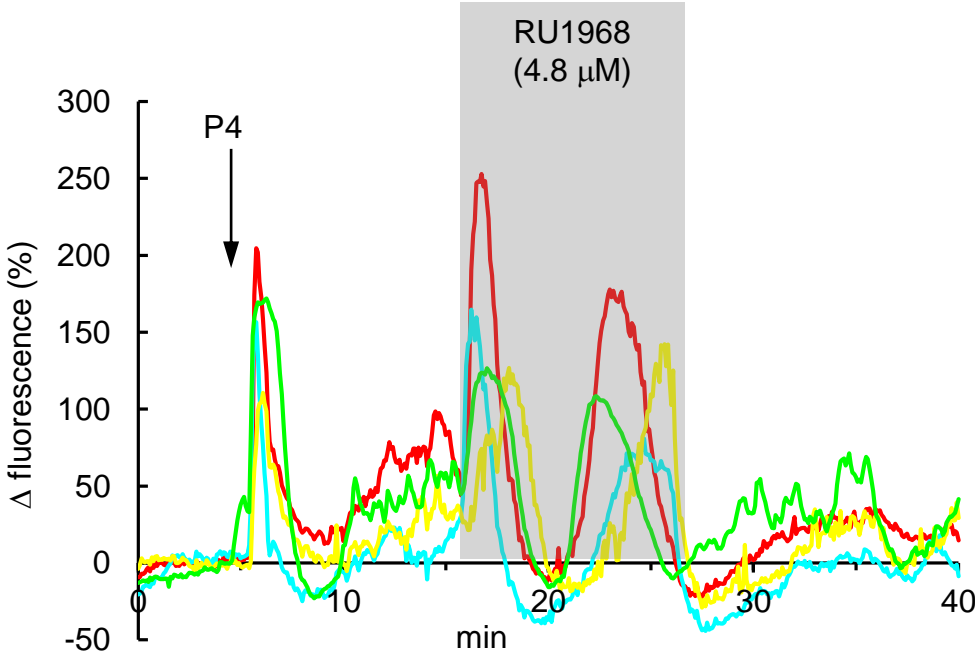


Fig S4